NASA TECHNICAL NOTE

NASA TN D-3725

NASA TN D-3725
c.1

FULL-SCALE WIND-TUNNEL INVESTIGATION OF A VTOL AIRCRAFT WITH A JET-EJECTOR SYSTEM FOR LIFT AUGMENTATION

by Jerry V. Kirk and David H. Hickey

Ames Research Center
Moffett Field, Calif.

NATIONAL AERONAUTICS AND SPACE ADMINISTRATION • WASHINGTON, D. C. • NOVEMBER 1966

Completed 20 Jul 67 GYR

ERRATA

NASA Technical Note D-3725

FULL-SCALE WIND-TUNNEL INVESTIGATION OF A VTOL AIRCRAFT WITH A JET-EJECTOR SYSTEM FOR LIFT AUGMENTATION

By Jerry V. Kirk and David H. Hickey

Page 29, Figure 13:

For $T_c = 1.2$, all data points are 1.00 C_L high. For example, at $\alpha = 0^\circ$, C_L should be 2.0 rather than 3.0.

NASA-Langley, 1967

Issued 6-8-67

NASA TN D-3725

FULL-SCALE WIND-TUNNEL INVESTIGATION OF A VTOL AIRCRAFT WITH A JET-EJECTOR SYSTEM FOR LIFT AUGMENTATION

By Jerry V. Kirk and David H. Hickey

Ames Research Center
Moffett Field, Calif.

NATIONAL AERONAUTICS AND SPACE ADMINISTRATION

For sale by the Clearinghouse for Federal Scientific and Technical Information
Springfield, Virginia 22151 – Price $2.00

FULL-SCALE WIND-TUNNEL INVESTIGATION OF A VTOL AIRCRAFT WITH A JET-EJECTOR SYSTEM FOR LIFT AUGMENTATION

By Jerry V. Kirk and David H. Hickey
Ames Research Center

SUMMARY

Aerodynamic characteristics of a VTOL aircraft incorporating a jet ejector for augmenting lift have been examined from hover up to and including wing-supported flight.

Ejector performance was measured statically and with forward speed. The maximum static augmentation ratio measured was 1.19. The ratio of ejector thrust with forward speed to static ejector thrust increased with forward speed.

In general, the aircraft had nearly neutral longitudinal stability at angles of attack below wing stall, but above wing stall, pitch-up was severe. Lateral and directional stability were positive. Control power for trim in transition appeared to be adequate except for recovering from post stall pitch-up. Results from tests in a full-scale wind tunnel, in flight, and in a small-scale wind tunnel generally agree well.

INTRODUCTION

Many concepts have been suggested for augmenting the lift of fixed wing aircraft for vertical take-off and landing. One concept is a jet ejector system such as that used for augmenting lift on the Lockheed XV-4A.

The full-scale aerodynamic characteristics of this aircraft and its ejector system were investigated in a wind tunnel at conditions ranging from hover up to and including conventional wing-supported flight. Ejector performance, longitudinal characteristics, lateral-directional stability and control, and control power about all three axes were determined at various airspeeds and control settings through the transition flight regime. The results are compared with those from flight tests (ref. 1) and from a small-scale wind tunnel (ref. 2).

NOTATION

A	ejector exit area, sq ft
b	wing span, ft

$\bar{c}$	mean aerodynamic chord, $\frac{2}{S}\int_{o}^{b/2} c^2\,dy$
C_D	drag coefficient, $\frac{D}{qS}$
C_l	rolling-moment coefficient, $\frac{l}{qSb}$
C_L	lift coefficient, $\frac{L}{qS}$
C_m	pitching-moment coefficient, $\frac{M}{qS\bar{c}}$
C_n	yawing-moment coefficient, $\frac{N}{qSb}$
C_y	side-force coefficient, $\frac{Y}{qS}$
D	drag, lb
l	rolling moment, ft-lb
L	total lift on aircraft, lb
m	mass flow, $\rho A v_j$, slugs/sec
M	pitching moment, ft-lb
N	yawing moment, ft-lb
P_o	standard atmospheric pressure, 2116 lb/sq ft
P_s	test section static pressure, lb/sq ft
P_{tp}	engine tail-pipe total pressure, in. Hg
q	free-stream dynamic pressure, lb/sq ft
R	Reynolds number
S	wing area, sq ft
T	complete ejector thrust in the lift direction, $\rho A v_j^2$, lb
T_c	thrust coefficient, $\frac{T}{qS}$

v	air velocity, ft/sec
V	free-stream velocity, knots
Y	side force, lb
α	angle of attack of the wing chord plane, deg
β	sideslip angle, deg
ρ	density, $lb\text{-}sec^2/ft^4$
δ	relative static pressure, $\frac{P_s}{P_o}$
δ_a	aileron deflection measured normal to the hinge line, left aileron down, positive, deg
δ_e	elevator deflection measured normal to the hinge line, trailing edge down, positive, deg
δ_f	flap deflection measured normal to the hinge line, deg
δ_r	rudder deflection measured normal to the hinge line, trailing edge right, positive, deg

Subscripts

e	ejector
j	ejector exit
s	static
u	uncorrected
α	variable angle of attack

AIRCRAFT DESCRIPTION

The Lockheed XV-4A is a twin-engined midwing monoplane incorporating a propulsion system and all controls necessary for vertical take-off and landing (VTOL) and for transition to conventional wing-supported flight. In figure 1 the aircraft is shown mounted on the normal strut system in the test section of the 40- by 80-foot wind tunnel. Figure 2 is a two-view drawing of the aircraft.

Propulsion System

The exhaust from two JT12A-3 turbojet engines, which is directed aft in the normal manner for conventional flight, is directed to a ducted manifold along the upper fuselage for VTOL and transition to wing-supported flight. The manifold has 40 elongated nozzles in 20 rows of 2 each (see fig. 1(a)). Each nozzle is canted 10° aft of the vertical plane. The flow of exhaust gases from the nozzles into mixing chambers in the fuselage provides ejector action. Doors above and below the ejectors are open during VTOL and transition flight.

The different propulsion configurations employed during transition from hover to wing supported flight studied were: Configuration I - exhaust from both engines being diverted to the ejector manifold; configuration II - one engine exhausting conventionally and one exhausting through the ejector manifold; configuration III - both engines exhausting conventionally, but with the ejector inlet and exit doors open (just prior to complete conversion to conventional flight).

Hover Controls

Aircraft attitude about all three axes is controlled with reaction jets during hover and low-speed flight. During VTOL operation, approximately 10 percent of the engine exhaust gas flows continuously to the pitch and yaw nozzles located in the nose and tail of the aircraft. For longitudinal control, the division of gas flow between the fore and aft nozzles is varied; for directional control, the nozzles in the nose and tail are swiveled in opposing directions. Engine compressor bleed air is supplied, on demand only, to roll-control valves on the upper and lower surface of each wing tip.

Boundary-Layer Control

The aircraft has blowing boundary-layer control over the leading edge of the horizontal stabilizer and elevators to prevent the air flow from separating and to increase control power during transition flight. Engine compressor bleed air was used for the BLC system. The BLC was on for all tests unless otherwise noted.

Conventional Controls

The aircraft has ailerons, a rudder, and elevators for conventional flight. Both the ailerons and rudder deflect $\pm 20^{\circ}$. The elevators have two control limits that differ with the flight configuration: For conventional flight the limits are $\pm 30^{\circ}$; during hover and transitional flight (configurations I and II), the limits are from 0° to 60°, trailing edge down. Neutral elevator for the transitional mode is approximately 26°, trailing edge down.

TESTING PROCEDURE

Six-component force and moment data were measured at angles of attack from -12° to $+28^{\circ}$. The static performance of the ejector augmentation system was measured with a force balance and a pressure and temperature rake mounted beneath the left-hand ejector bay. Thermocouples and pressure transducers on the rake provided the data needed to calculate the mass flow.

For most of the tests half power was used because the life of the ejector primary nozzle was limited at full power. The data are presented in terms of thrust coefficient so that the results can be adjusted to other power conditions. Airspeed was varied from 0 to 100 knots; at the highest speed, Reynolds number was 4.7 million.

Tests at Constant Angle of Attack

Power, angle of sideslip, and longitudinal, lateral, and directional control settings were varied at a constant angle of attack. The angle of attack was varied with airspeed so as to obtain data for thrust nearly equal to drag. Aircraft configurations I and II were studied in this manner.

Ejector thrust was measured for a representative combination of power settings and angles of attack.

Variable-Angle-of-Attack Testing

Configuration variables and airspeed were held essentially constant while angle of attack was varied. For the majority of tests, the angle of attack was first set for zero drag with longitudinal control set to trim pitching moment near zero. Angle of attack was then varied. In most instances the angle-of-attack range included the maximum nose-down longitudinal control available.

Corrections to Data

Force and moment data for the conventional configuration (jet augmentation system not operating) were corrected for the effects of wind-tunnel wall interference in the following manner:

$$\alpha = \alpha_u + 0.2679C_{L_u}$$

$$C_D = C_{D_u} + 0.0047C_{L_u}^2$$

$$C_m = C_{m_u} + 0.0103C_{L_u}$$

No corrections were applied to the data for the transition configuration (jet augmentation system operating) since the effect of ejector air flow on wind-tunnel wall corrections was not known.

A major part of the test program was run with no fairing on the tail strut. Appropriate drag tare corrections have been applied to the data to account for the tail strut drag. Near the end of the program, a fairing was placed over the tail strut as a check on the validity of the corrections. The results agree within the accuracy of the measurements.

RESULTS

Table I is an index to the figures. In general the low speed configuration I results are referenced to static thrust at hover.

Propulsion System Performance

Static thrust of the aircraft is shown in figure 3(a). Unflagged symbols include the thrust from the pitch reaction controls, while the flagged symbols are measurements of ejector thrust only. The effect of forward speed on ejector performance (from pressure measurements) is shown in figure 4. The results in figure 4 are calculated from pressure and temperature measurements.

Aerodynamic Characteristics

The variation in aircraft longitudinal characteristics with forward speed for two configurations and two power settings is shown in figure 5. Also shown is a comparison of ejector thrust with measured aircraft lift.

Figures 6 through 13 present the variation in aircraft longitudinal characteristics with angle of attack. Figures 14 and 15 show the pitching-moment variation with angle of attack for various longitudinal control settings, power settings, and forward speeds. These results are taken from figures 9 through 13.

The variation in lateral-directional characteristics at constant angle of attack is shown in figures 16 and 17.

Control Power

Figures 18 through 21 show the longitudinal control power available both with and without the boundary-layer control operating over the horizontal tail.

Lateral control power of the XV-4A is shown in figures 22 through 24, and directional control power in figures 25 through 30.

DISCUSSION

Ejector and Airplane Performance

Zero speed.- The maximum static thrust measured was 6400 pounds (fig. 3). This value includes the unaugmented thrust from the pitch reaction controls. Engine thrust in the conventional configuration at the same engine pressure ratio was 5450 pounds. Subtracting the unaugmented thrust gives an augmentation factor for the ejector of 1.19. Mass flow calculated for the maximum thrust condition was 15.8 slugs per second corresponding to a weight rate of flow of approximately 500 pounds per second. The weight rate of flow to the ejector for the two JT12A-3 gas generators is approximately 90 pounds per second; therefore the flow augmentation ratio of the ejector was about 5.5 to 1.

Forward speed.- The ratio of ejector thrust to static ejector thrust increased with forward speed for configuration I (fig. 4). Agreement is good for the three power settings shown. The low and high power results in figure 5(a) for configuration I correlate well except for the high power, high thrust coefficient results for lift. Figure 5(b) shows the measured aircraft lift to static thrust ratio compared with ejector thrust and ejector thrust plus power off wing lift. There is positive induced lift for the entire thrust coefficient range shown. No lift droop with forward speed is apparent. At 50 knots (T_c = 7 full scale) the measured lift to static thrust value represents about a 15-percent overload capability for STOL operation.

Configuration II results (fig. 5(c)) are also presented as the ratio of forces and moments to static thrust. Good correlation is shown for the low and high power settings.

Stability and Control

Longitudinal stability and control.- For configuration I static longitudinal stability throughout the transition from hover to wing-supported flight was neutral to slightly unstable (see fig. 14). The pitching-moment curve was fairly linear and no pitch-up problems were apparent in the angle-of-attack range below stall for speeds up to 70 knots. Configuration II has a pronounced nose-down pitching-moment variation with airspeed below a thrust coefficient of approximately 1.4 (fig. 5(c)). This pitch-down is probably due to decreased ejector effectiveness (decreased mass flow through the ejector due to ejector inlet flow separation) and to increased trailing-edge flap contribution to pitching moment as forward speed is increased.

The fixed incidence horizontal tail of the XV-4A is mounted above the vertical tail (T type). The aircraft was tested far above the stalling angle of attack with longitudinal controls set near trim and with full nose-down control (aerodynamic plus reaction) to examine the longitudinal stability and control in the deep stall region. Wind-tunnel results indicate that at low speeds (approximately 25 to 35 knots) there is sufficient control to trim

the aircraft through the maximum angle of attack tested (28°), although pitch-up occurs between 16° and 20°, depending on forward speed (figs. 14(a) and (c)). At higher forward speeds control is not sufficient to trim the pitching moment at the higher angles of attack. At approximately 55 knots (scaling the results to full power conditions), the angle of attack beyond which the aircraft cannot be trimmed is approximately 26° (fig. 14(c)), while at approximately 70 knots the maximum angle of attack for trim is 18° (fig. 14(d)).

Control effectiveness is significantly decreased at elevator deflection angles above 40° (figs. 19 through 21) for configurations I and II both with and without the horizontal-tail boundary-layer control system operating.

Lateral stability and control.- Lateral stability was positive for all configurations and angles of attack examined. Dihedral effect at low airspeeds is positive, but as forward speed is increased, the dihedral effect decreases (see fig. 17).

Lateral control power for configuration I is not symmetric (figs. 23 and 24) because one of the roll control valves malfunctioned in the right wing down position.

Directional stability and control.- Directional instability for configuration III at 8° angle of attack (fig. 16) is probably caused by the flow over the vertical fin being effectively blocked by the wing, large fuselage-mounted engine nacelles, and the ejector inlet and exit doors as angle of attack is increased. Configuration I (see fig. 17) had positive directional stability. Directional control power results show no unusual characteristics for the conventional configuration and for configuration I (figs. 25 through 30).

Comparison of Full-Scale Wind-Tunnel Results With Flight-Test and Small-Scale Results

Correlation of full-scale wind-tunnel and flight tests.- Figure 31 presents a comparison between results from the 40- by 80-foot wind tunnel and flight tests. Flight-test data were very limited and the results shown are from a decelerating transition. Angle of attack compares very favorably, the discrepancy being on the order of 1°. Elevator deflection for trim disagrees by 5° to 7°. The reason for this discrepancy is not fully understood, but the results from wind-tunnel measurements and flight tests were obtained from two different aircraft, and possible rigging differences could account for some of the discrepancy. The aircraft tested in the wind tunnel had been flown conventionally and hovered but had never been flown through a transition.

Comparison between full-scale and small-scale (18-percent) model results.- Data for an 18-percent scale model of the XV-4A (ref. 1) are compared with full-scale data in figure 32. All full-scale data were corrected to the same

thrust coefficient as the small-scale results. The effects of reaction control were subtracted from the full-scale results because the small-scale model did not have reaction controls. The results agree up to 4° angle of attack. Above 6° angle of attack the small-scale lift and moment results differ markedly from the full-scale results.

SUMMARY OF RESULTS

A full-scale wind-tunnel investigation of a VTOL aircraft incorporating a jet ejector for lift augmentation has shown:

1. The maximum static thrust augmentation ratio is 1.19 with a flow augmentation ratio of approximately 5.5.

2. The ratio of ejector thrust with forward speed to static ejector thrust increased with forward speed for configuration I.

3. Positive lift is induced for the entire thrust coefficient range in configuration I.

4. Longitudinal control at high angles of attack (beyond $C_{L_{max}}$) and forward speeds above 55 knots in configuration I was not sufficient for trimming the aircraft.

5. The dihedral effect at low forward speeds is positive but decreases as forward speed is increased.

6. Directional instability was apparent as angle of attack was increased in the phase III configuration.

7. Results from full-scale wind-tunnel tests, flight tests, and small-scale wind-tunnel tests generally agreed favorably.

Ames Research Center
National Aeronautics and Space Administration
Moffett Field, Calif., Aug. 16, 1966
721-01-00-08-21

REFERENCES

1. Cook, Woodrow L., and Hickey, David H.: Comparison of Wind-Tunnel and Flight-Test Aerodynamic Data in the Transition-Flight Speed Range for Five V/STOL Aircraft. NASA SP-116, Paper No. 26, 1966, pp. 447-467.

2. Barnes, O. G.: The VZ-10 Hummingbird 0.18 Scale Model Wind Tunnel Test Results. Lockheed ER-5623, April 1962.

TABLE I.- LIST OF FIGURES

Figure	Configuration	Remarks	Configuration variables						
			V, knots	α, deg	β, deg	δ_e, deg	δ_a, deg	δ_r, deg	δ_f, deg
3	I,II	Static aircraft performance	0	-12,0,12	0	26	0	0	40
4	I	Ejector performance with airspeed	Variable	0		26			
5	I,II	Aircraft longitudinal characteristics with airspeed	Variable	-6,0,6		30			
6	Conventional	Power-off longitudinal characteristics	40,80	Variable		0,26			0,40
7	III		80			0			40
8	Conventional	Power-on longitudinal characteristics							
9	I		20			33			
10			30			28,31,52			
11			40,50			30,52			
12			50,70			30,20			
13	II		50,67 85,100			30,24			
14	I	Longitudinal stability during transition	20 through 70			20 through 52			
15	II		50,67 85,100			30,24			
16	Conventional, III	Lateral-directional characteristics	80	0,8	Variable	0,-18			0,40
17	I		30,40,50	-2,-6,-8		28,40,33			40
18	Conventional	Longitudinal control power	80	0	0	Variable			0,40
19	I		0,20,30	0,12,20					40
20	I		40,50,70	-6,0,10, 20					
21	II		50,67,85 100	0,8					
22	Conventional	Lateral control power	80	0	-8,0	-18	Variable		0,40
23	I		0,30	0,12	0	25			
24	I		40,50	0	0	40,30			
25	Conventional	Directional control power	80	0	-8,0	-18	0	Variable	0,40
26	I		0	12	0	25			40
27	I		20	0	-10,0	28			
28	I		30		-10,0	25,28			
29	I		40		-6,0	40			
30	I		50		-8,0	33,30			
31	I	Comparison between full-scale wind-tunnel and flight-test results	Variable	Variable	---	Variable	---	---	
32	I	Comparison between full-scale and small-scale wind-tunnel results	---	Variable	0	0	0	0	

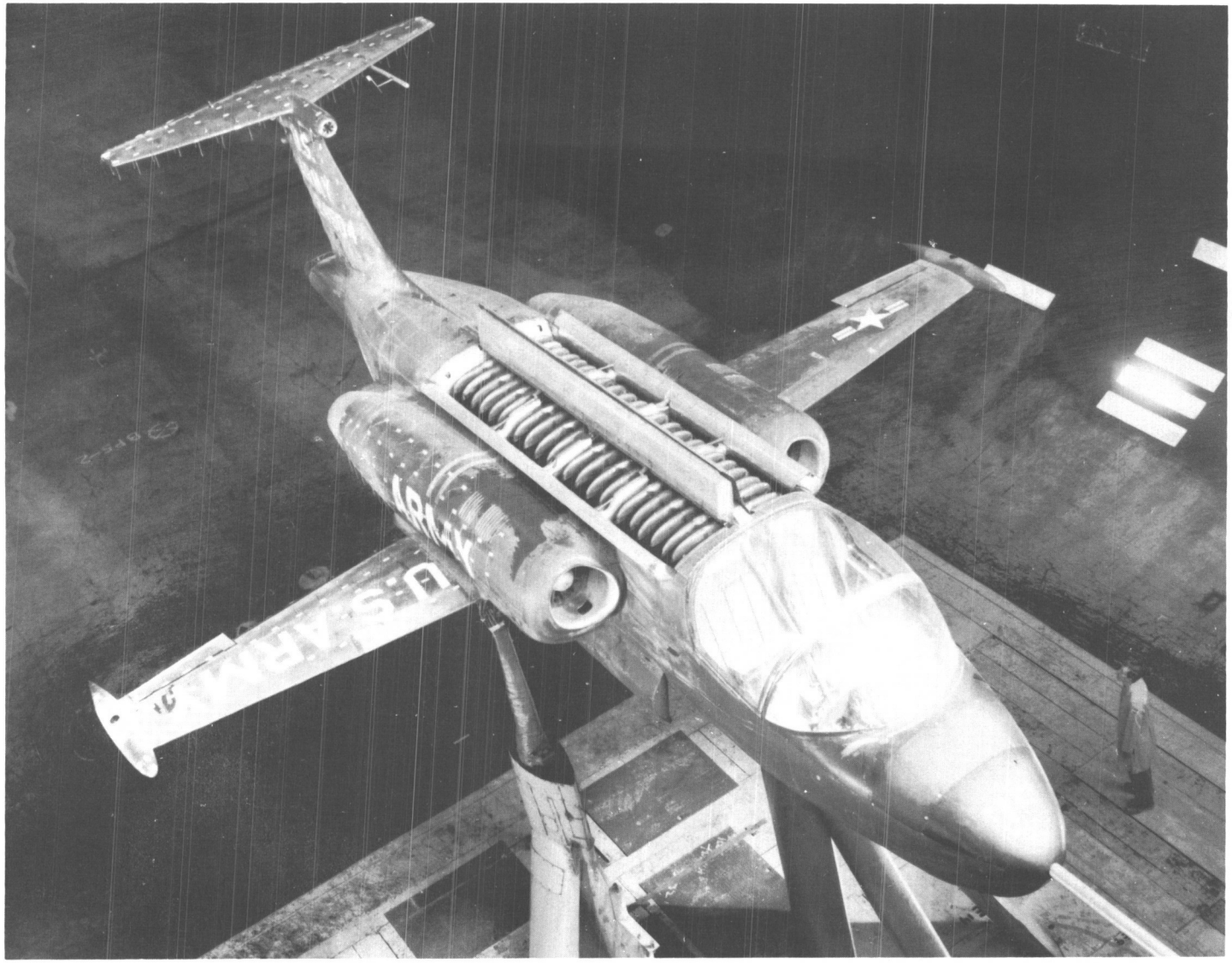

A-33193

(a) Overhead view showing ejector manifold.

Figure 1.- Photographs of the XV-4A mounted in the Ames 40- by 80-foot wind tunnel.

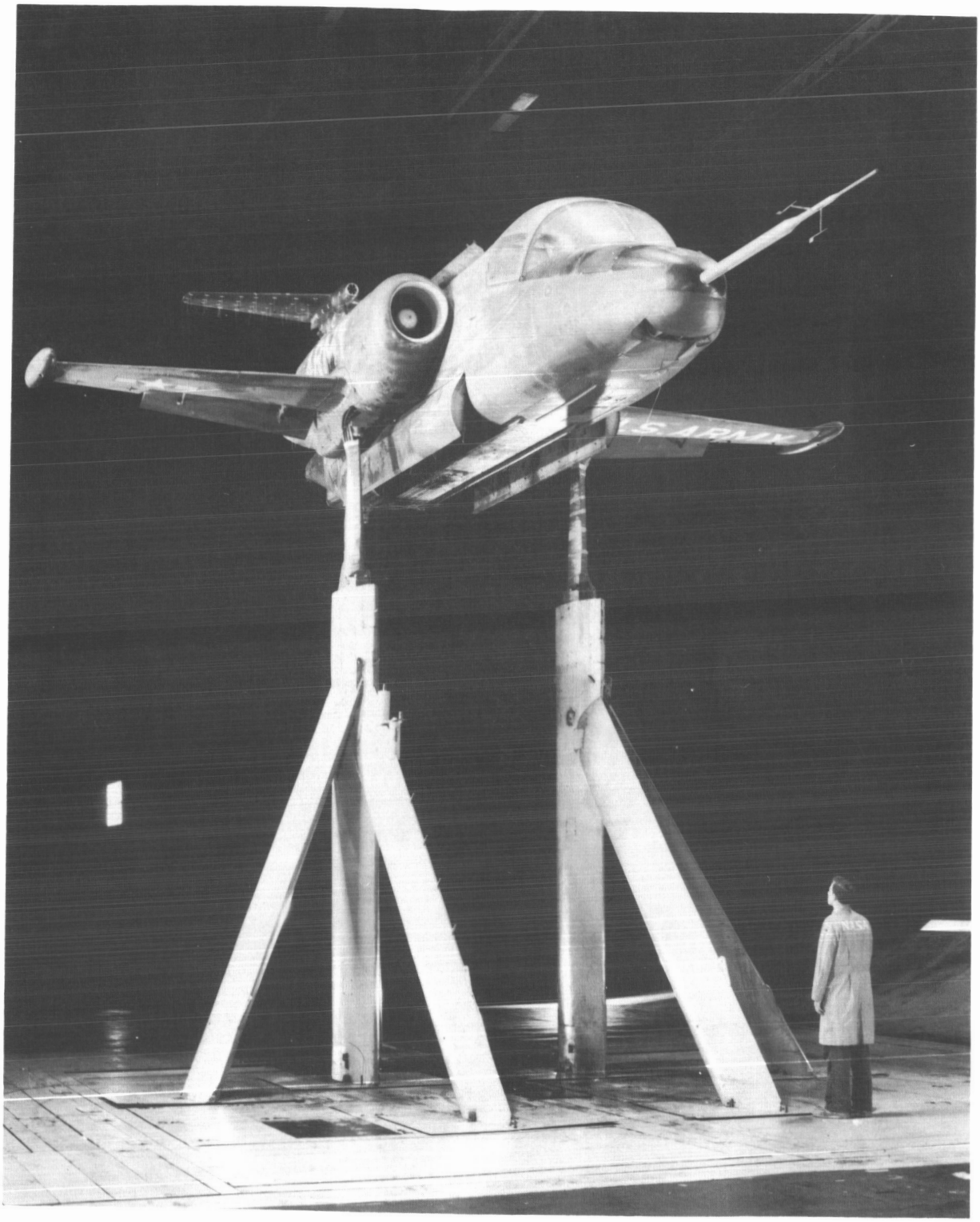

(b) Three-quarter front view. A-33194

Figure 1.- Concluded.

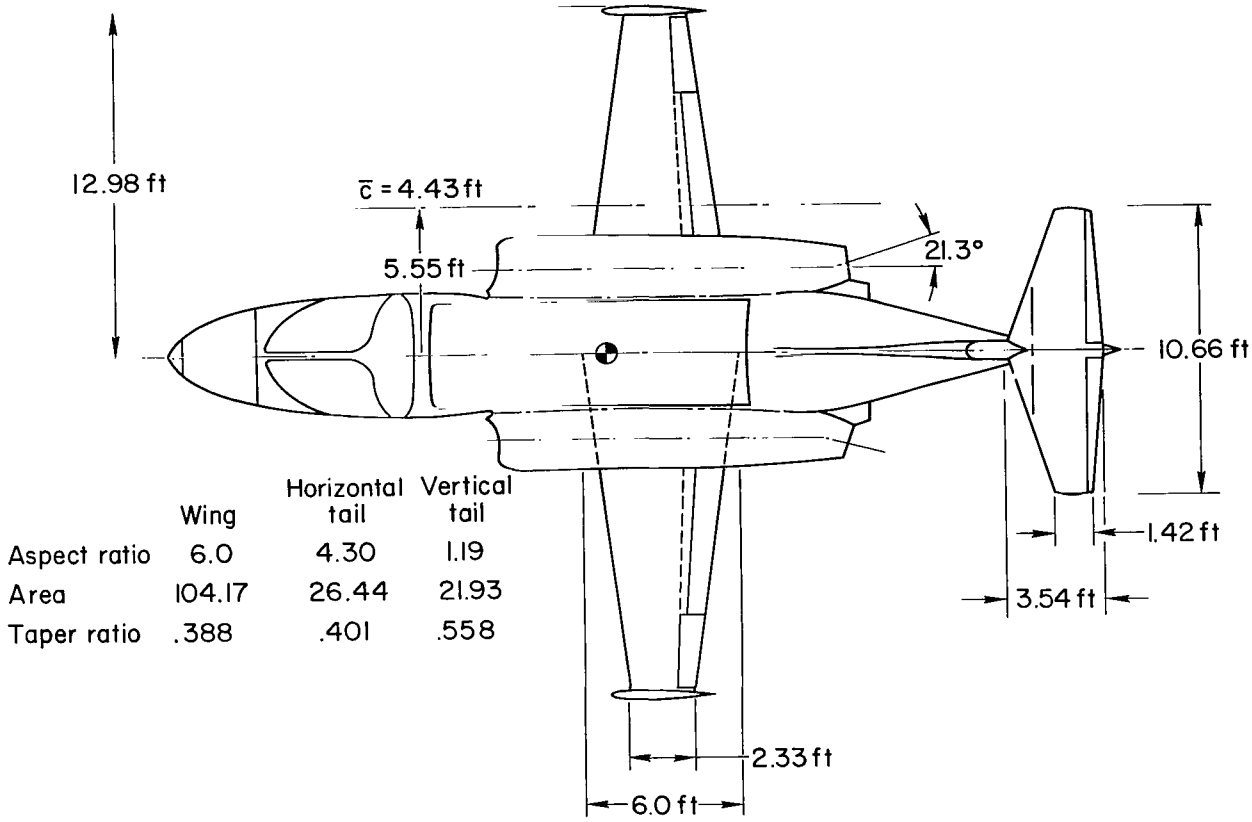

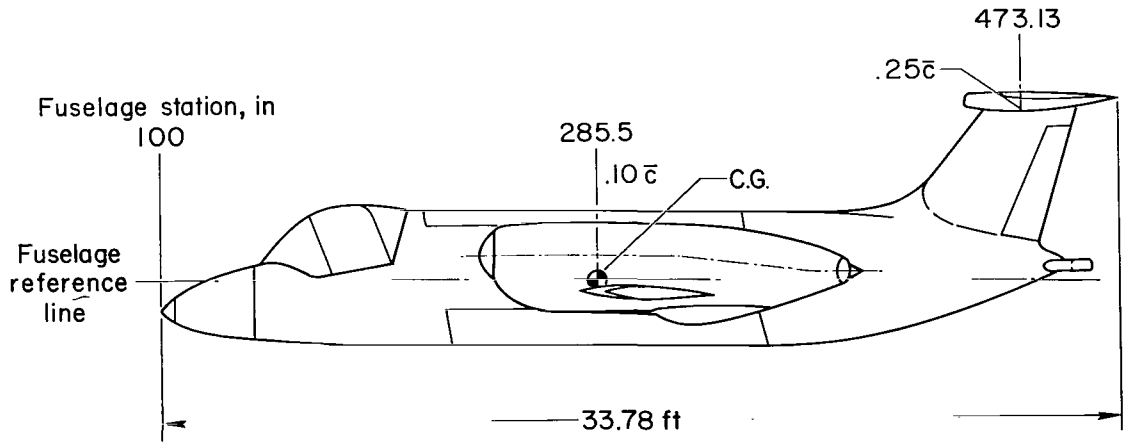

Figure 2.- General arrangement of the Lockheed XV-4A Hummingbird.

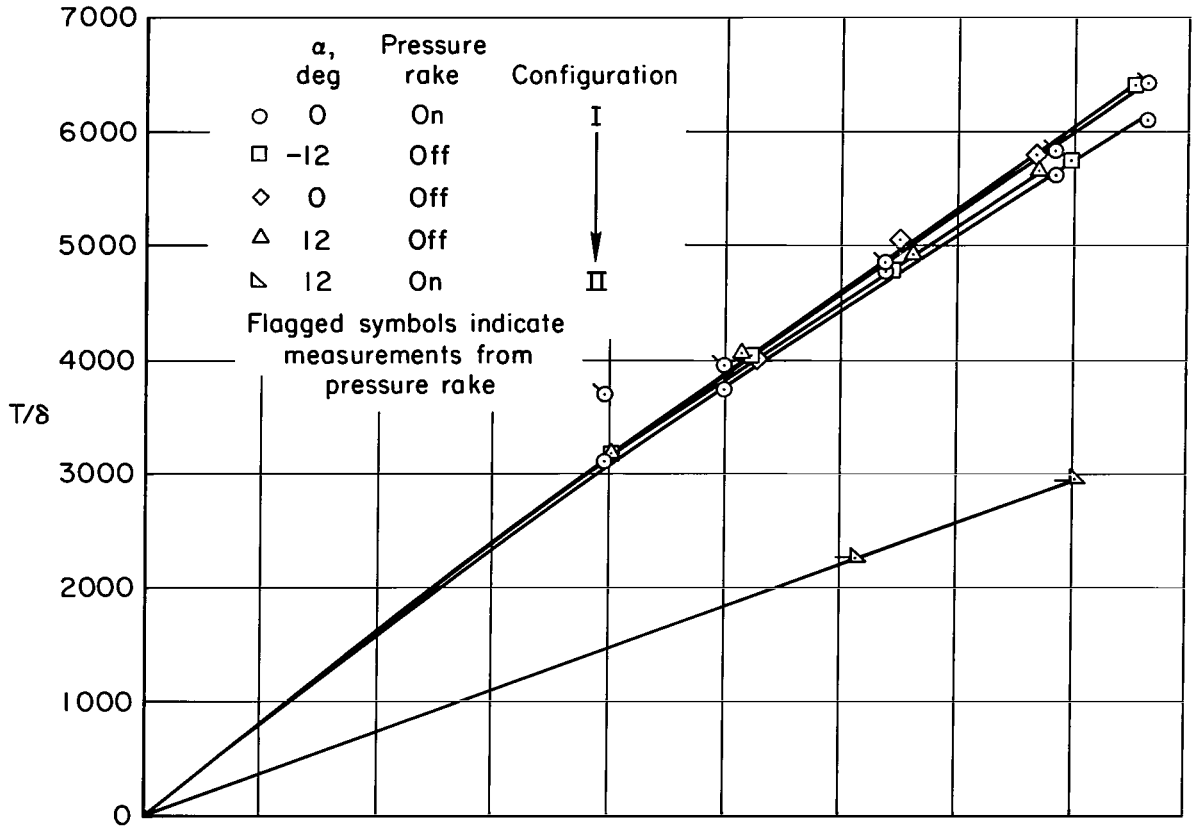

(a) Static thrust.

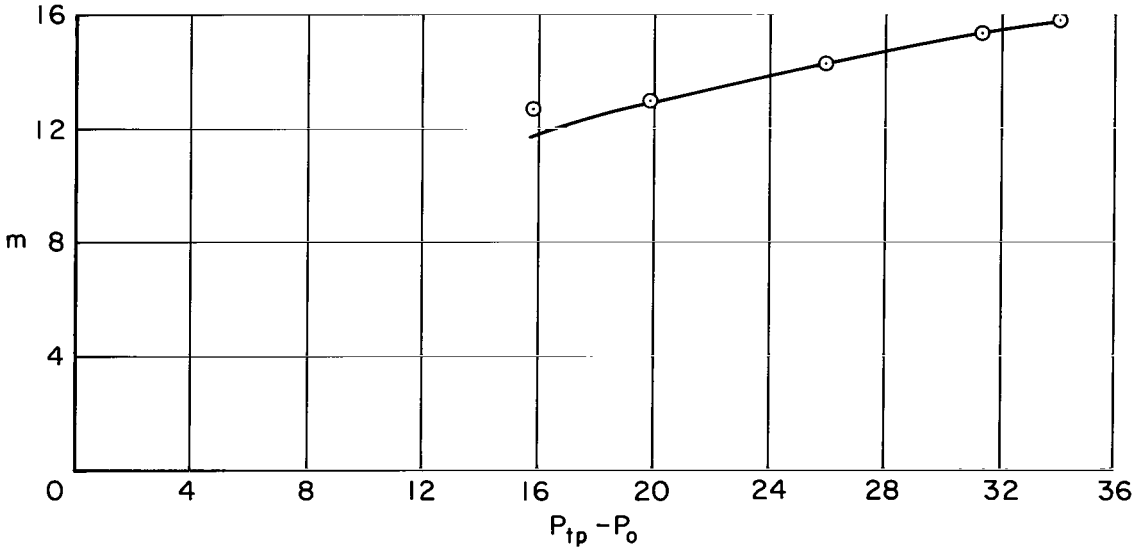

(b) Static mass flow, $\alpha = 0^{\circ}$.

Figure 3.- Zero airspeed performance of the aircraft.

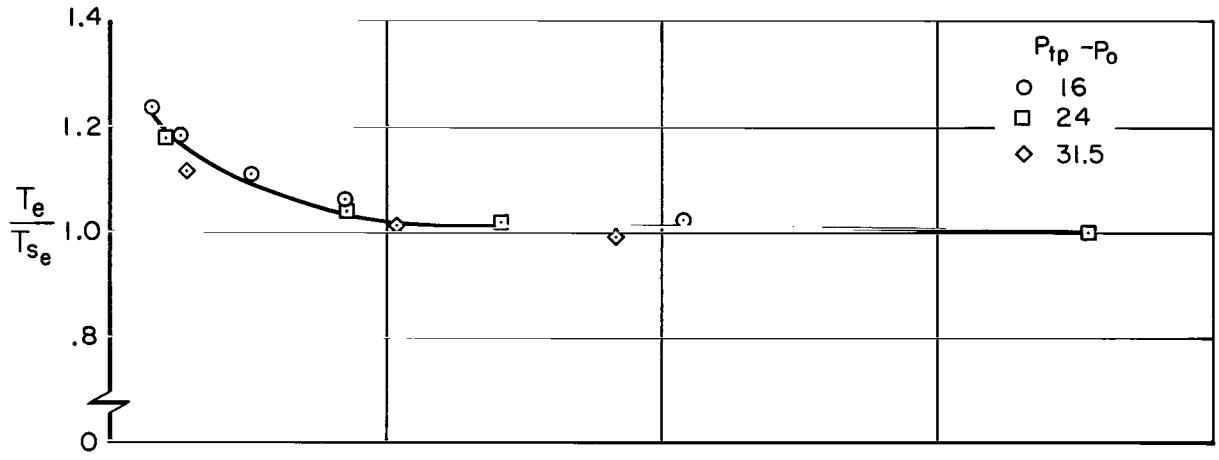

(a) Ejector thrust as measured by pressure rake.

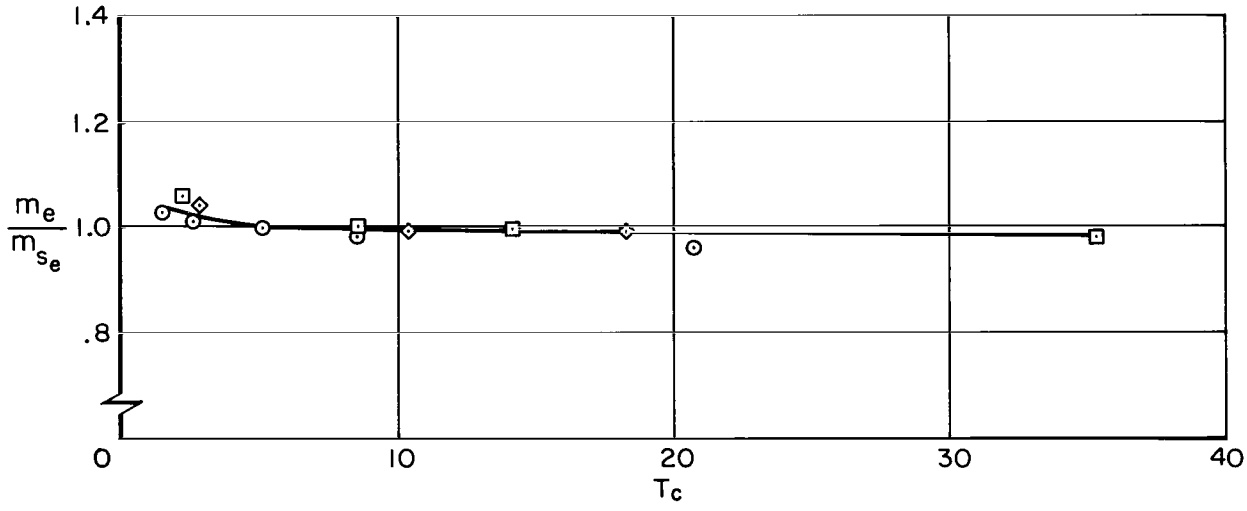

(b) Ejector mass flow.

Figure 4.- Ejector performance with airspeed and power setting; $\alpha = 0^{\circ}$.

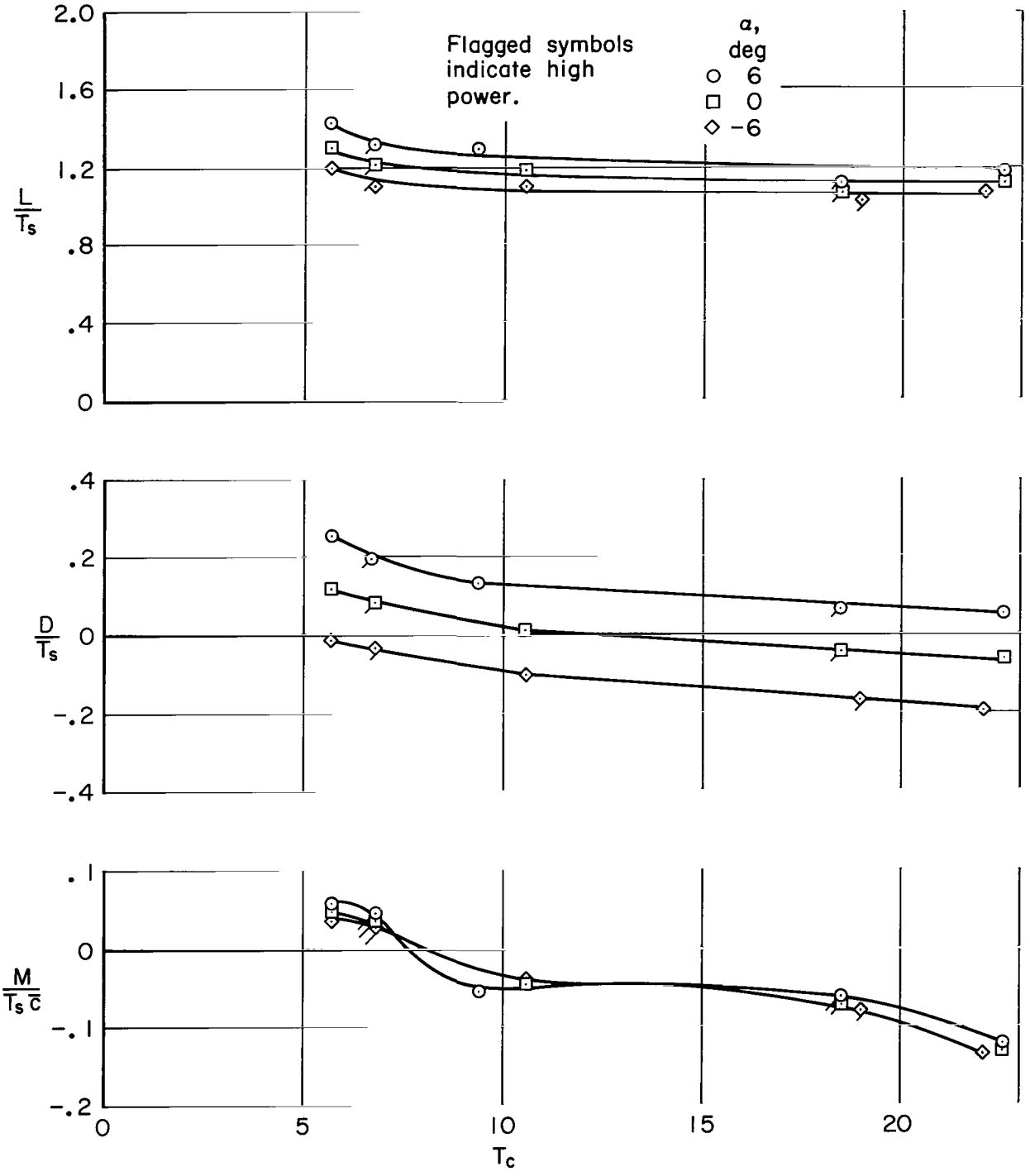

(a) Configuration I.

Figure 5.- Aircraft longitudinal characteristics with forward speed; $\delta_e = 30^\circ$, $\delta_f = 40^\circ$.

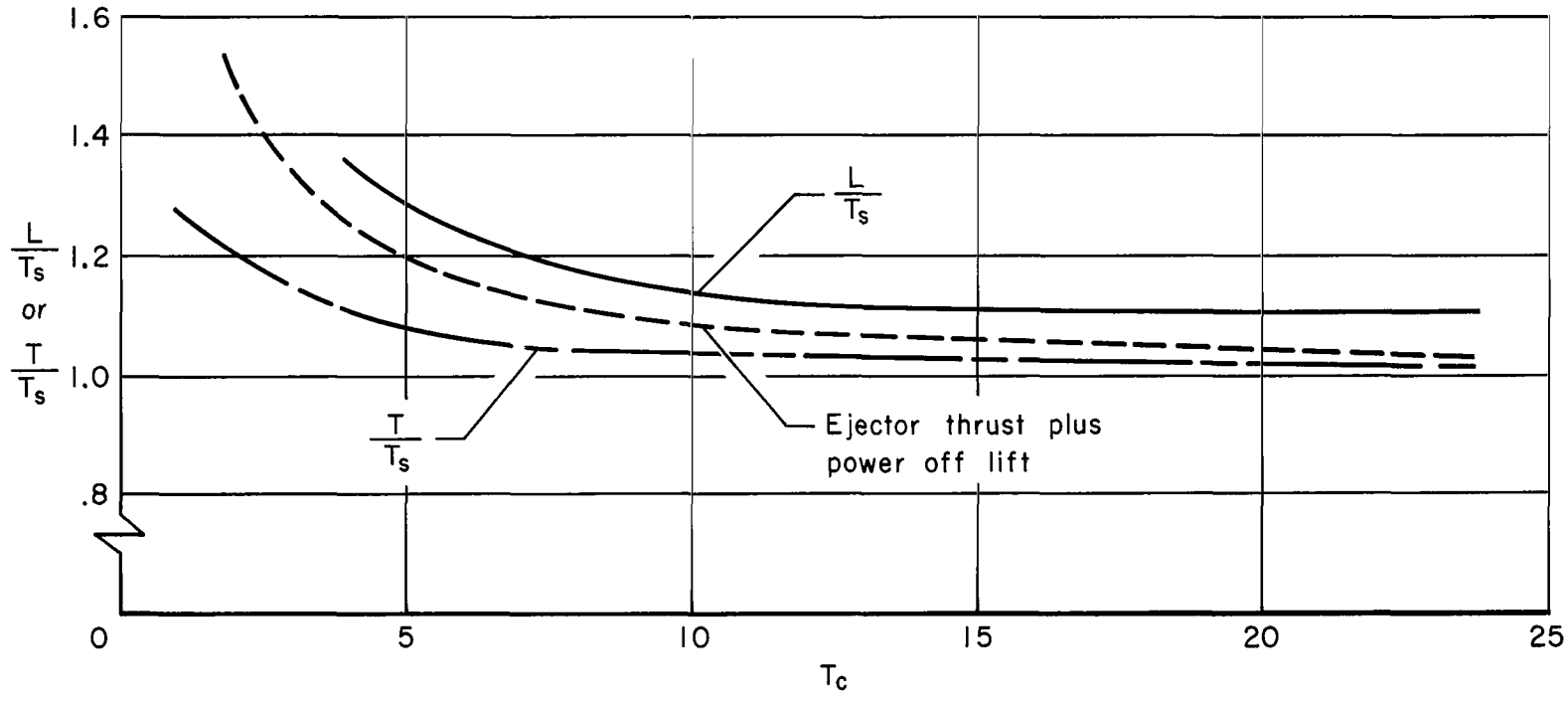

(b) Comparison of ejector thrust with measured aircraft lift; configuration I, $\alpha = 0^{\circ}$.

Figure 5.- Continued.

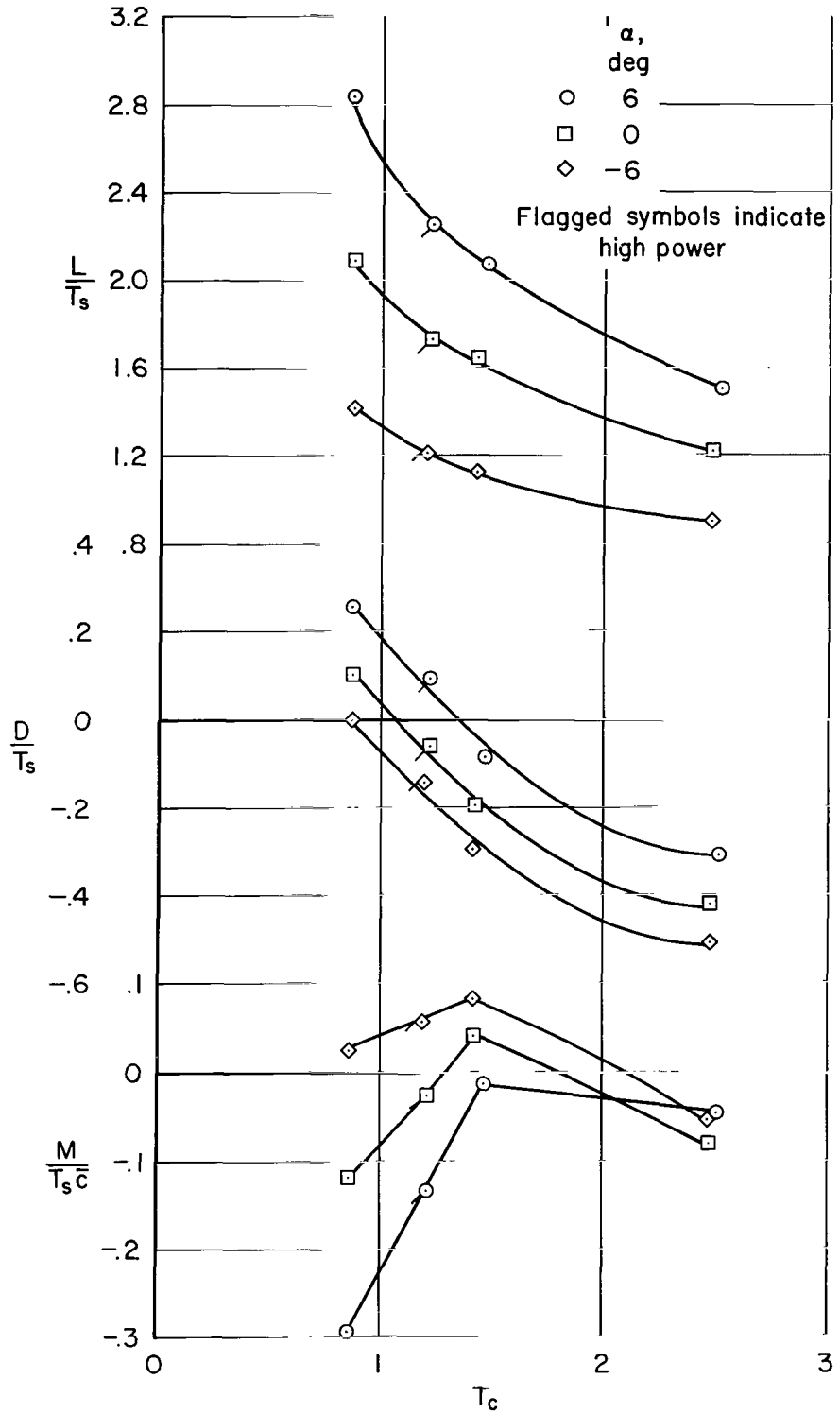

(c) Configuration II.

Figure 5.- Concluded.

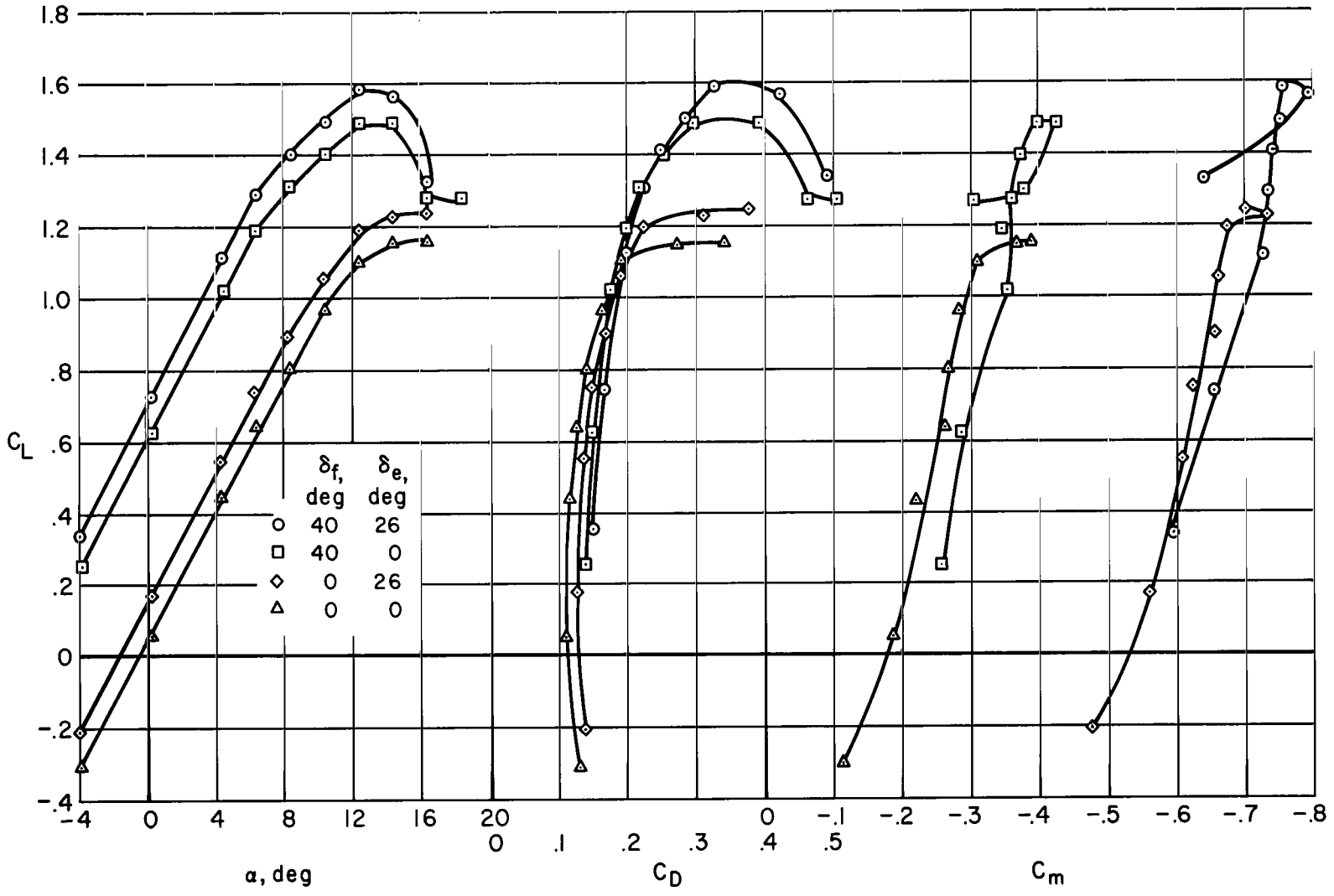

(a) Effect of flap position and elevator setting; V = 80 knots.

Figure 6.- Longitudinal characteristics with power off, conventional flight configuration.

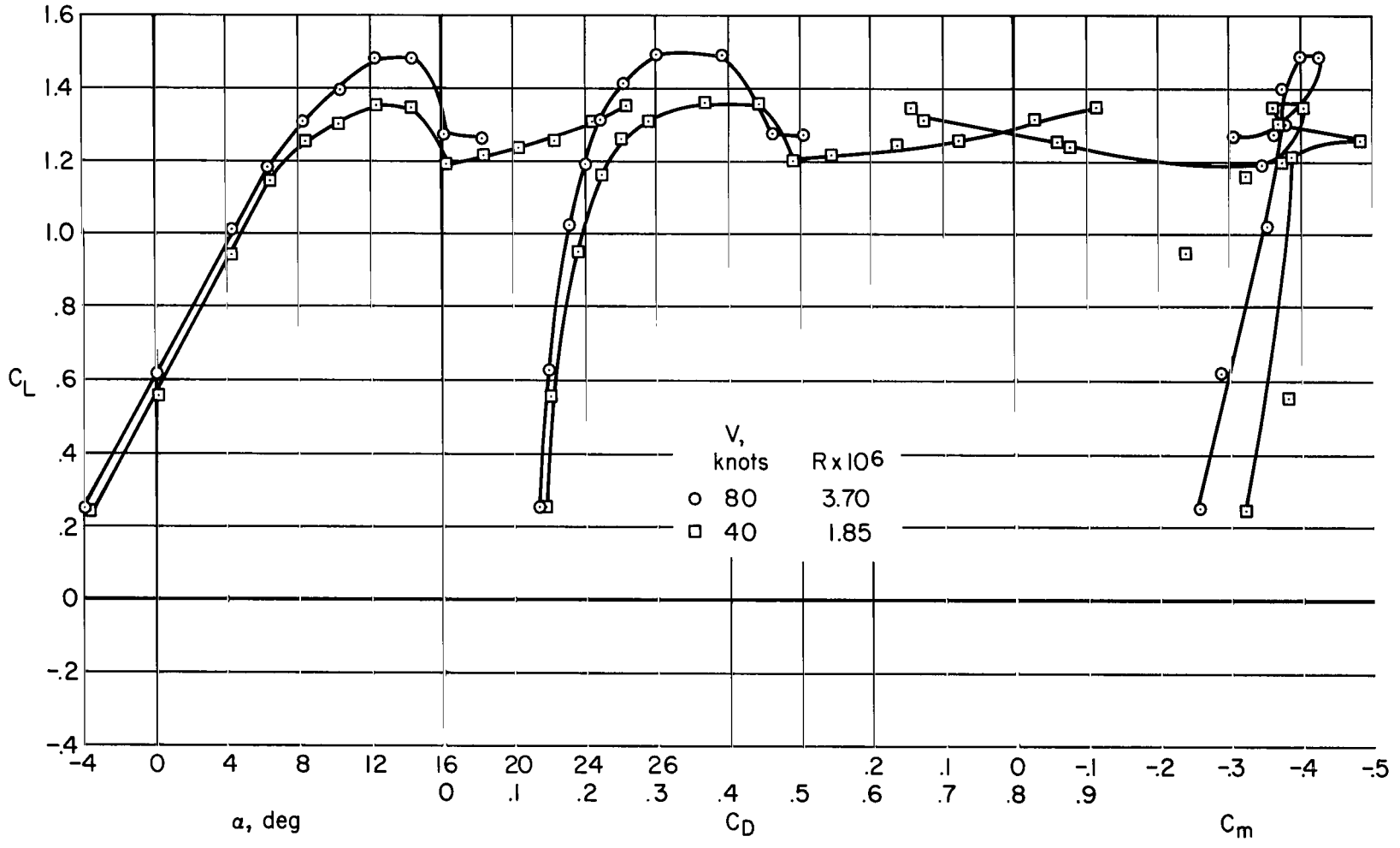

(b) Reynolds number effect; $\delta_e = 0^\circ$, $\delta_f = 40^\circ$.

Figure 6.- Concluded.

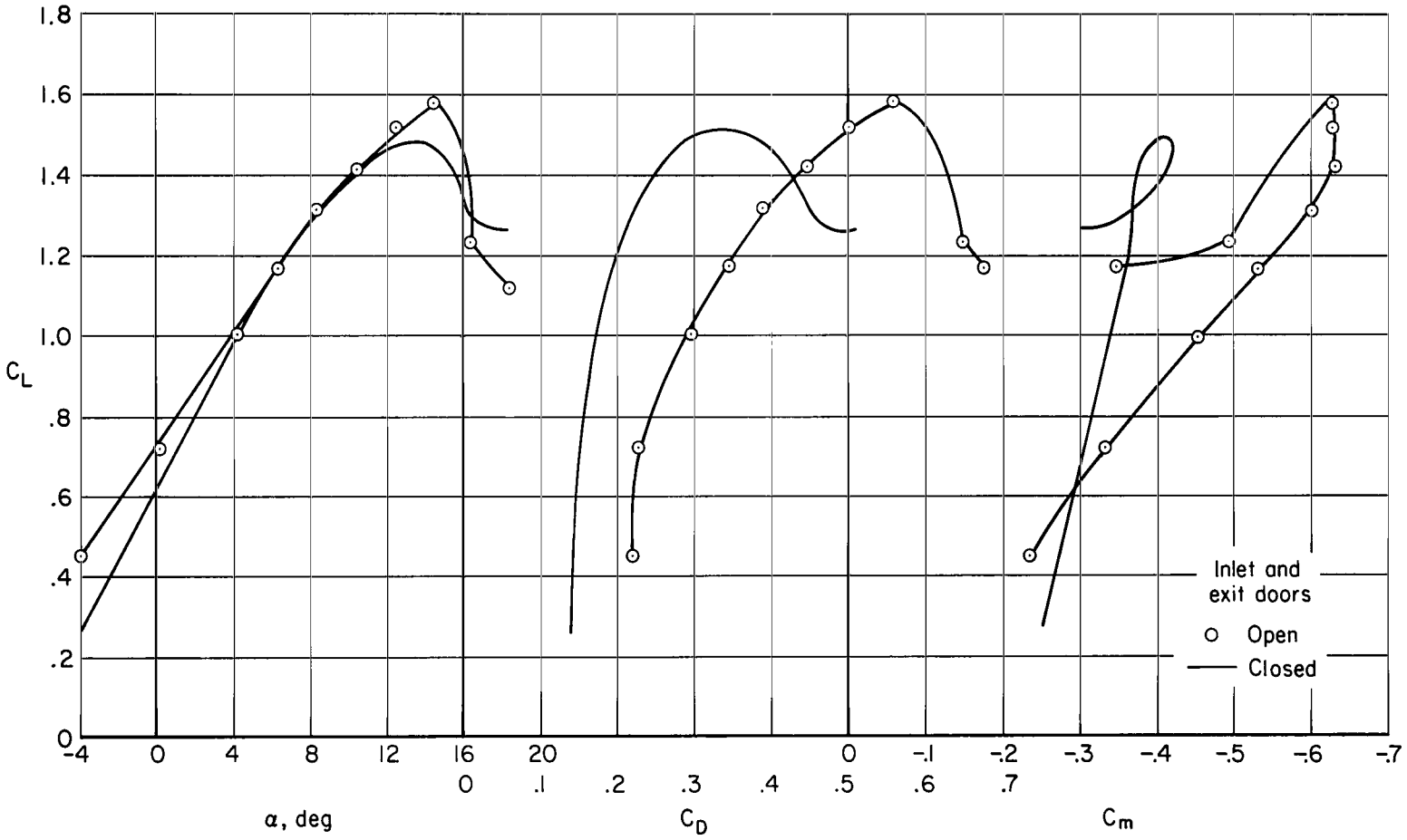

Figure 7.- Longitudinal characteristics in the preconversion configuration; power off, $\delta_e = 0^\circ$, $\delta_f = 40^\circ$, V = 80 knots.

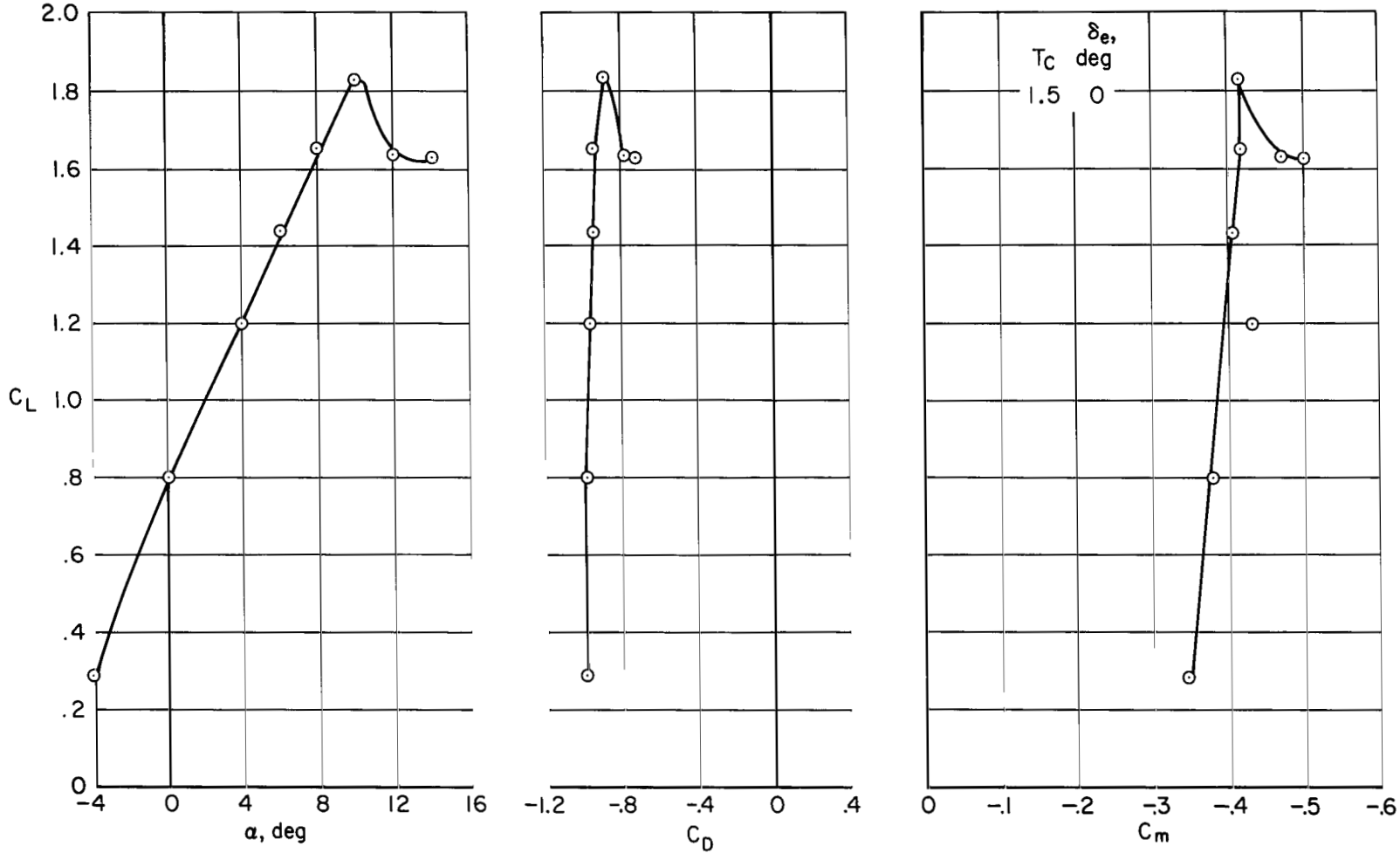

Figure 8.- Longitudinal characteristics in the conventional flight configuration with power on; low power, $\delta_e = 0^\circ$, $\delta_f = 40^\circ$, V = 80 knots.

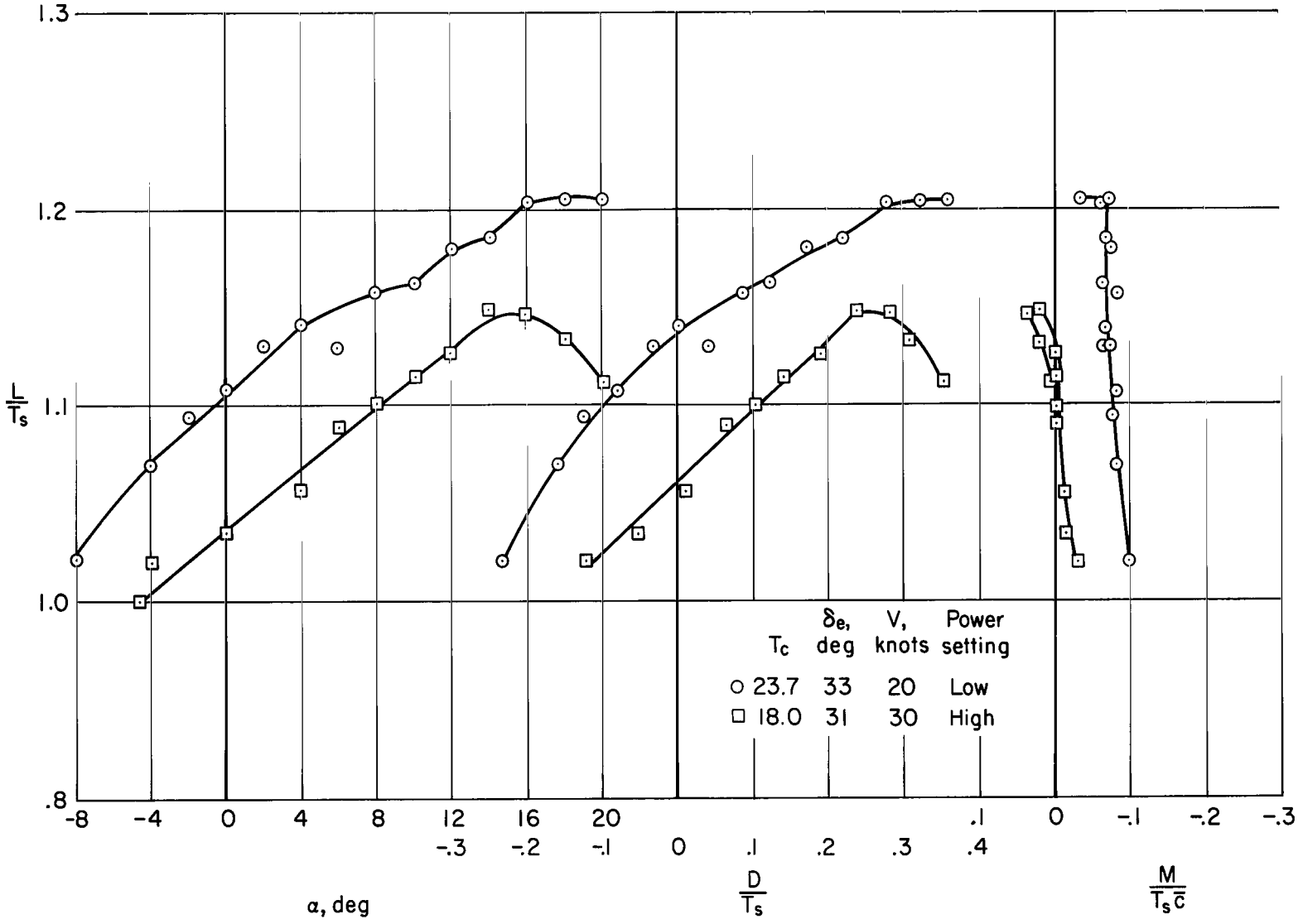

Figure 9.- Longitudinal characteristics in transition; configuration I, $\delta_f = 40^\circ$.

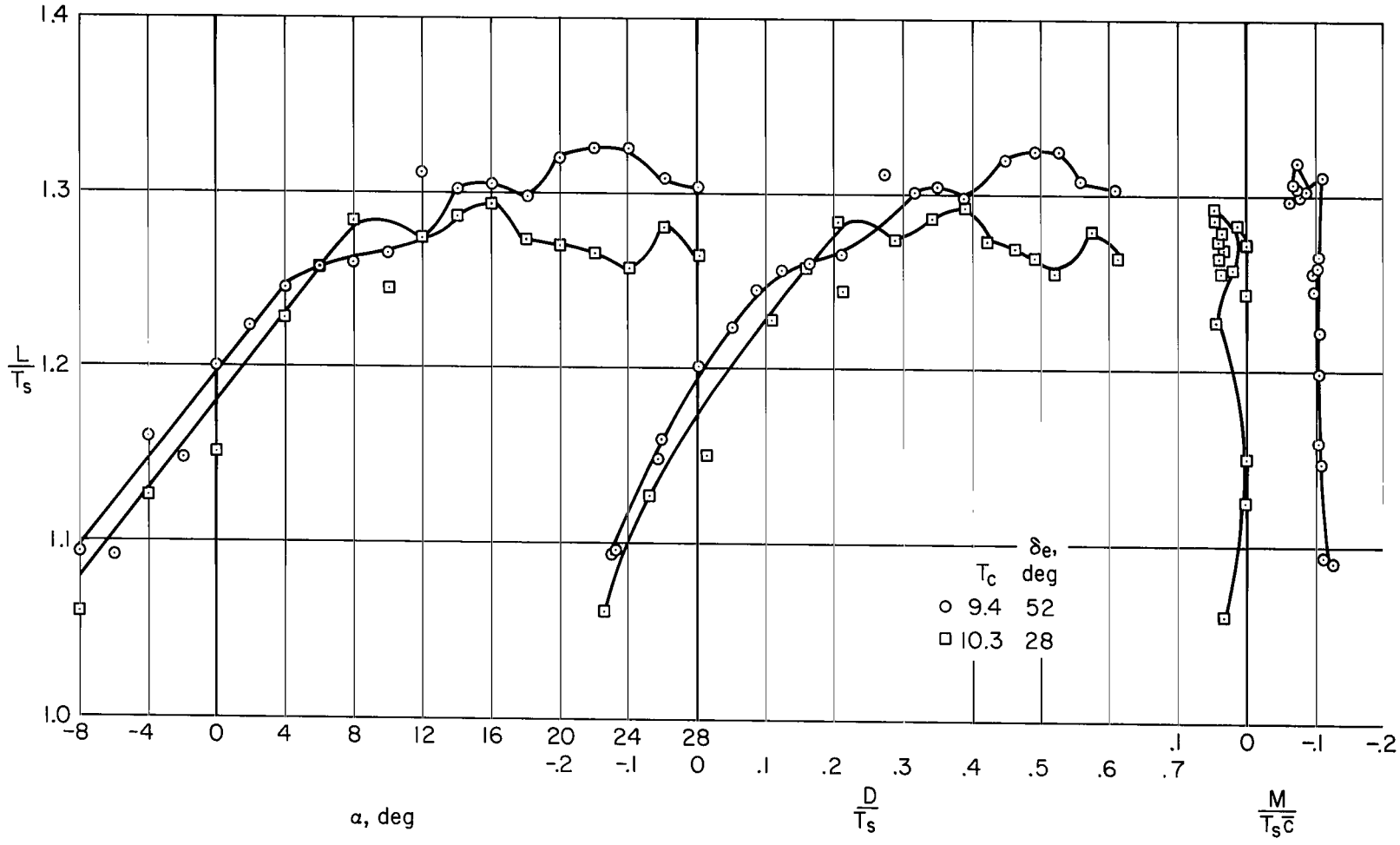

Figure 10.- Longitudinal characteristics in transition; configuration I, low power, $\delta_f = 40°$, V = 30 knots.

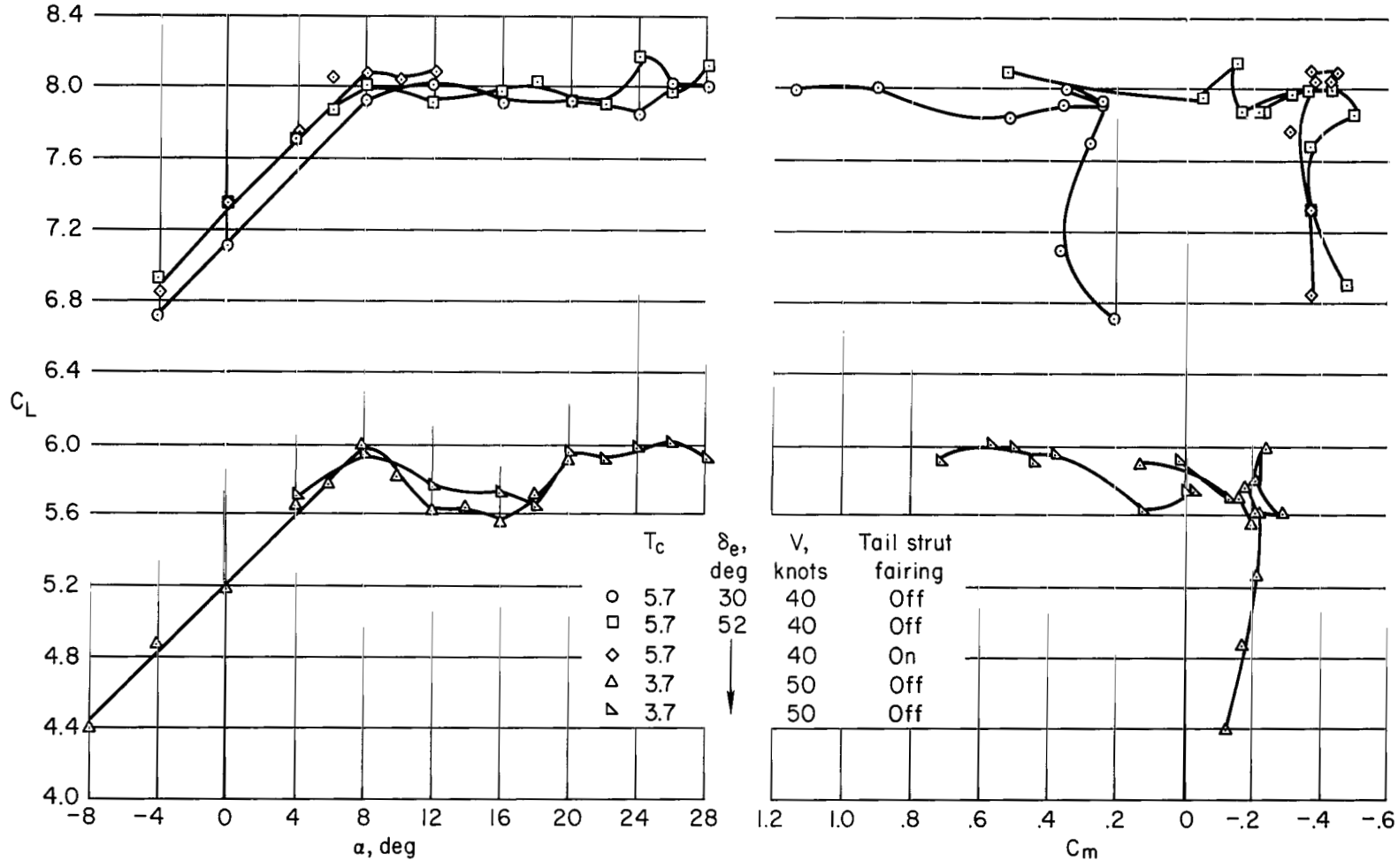

(a) C_L vs α and C_m

Figure 11.- Longitudinal characteristics in transition; configuration I, low power, $\delta_f = 40^\circ$.

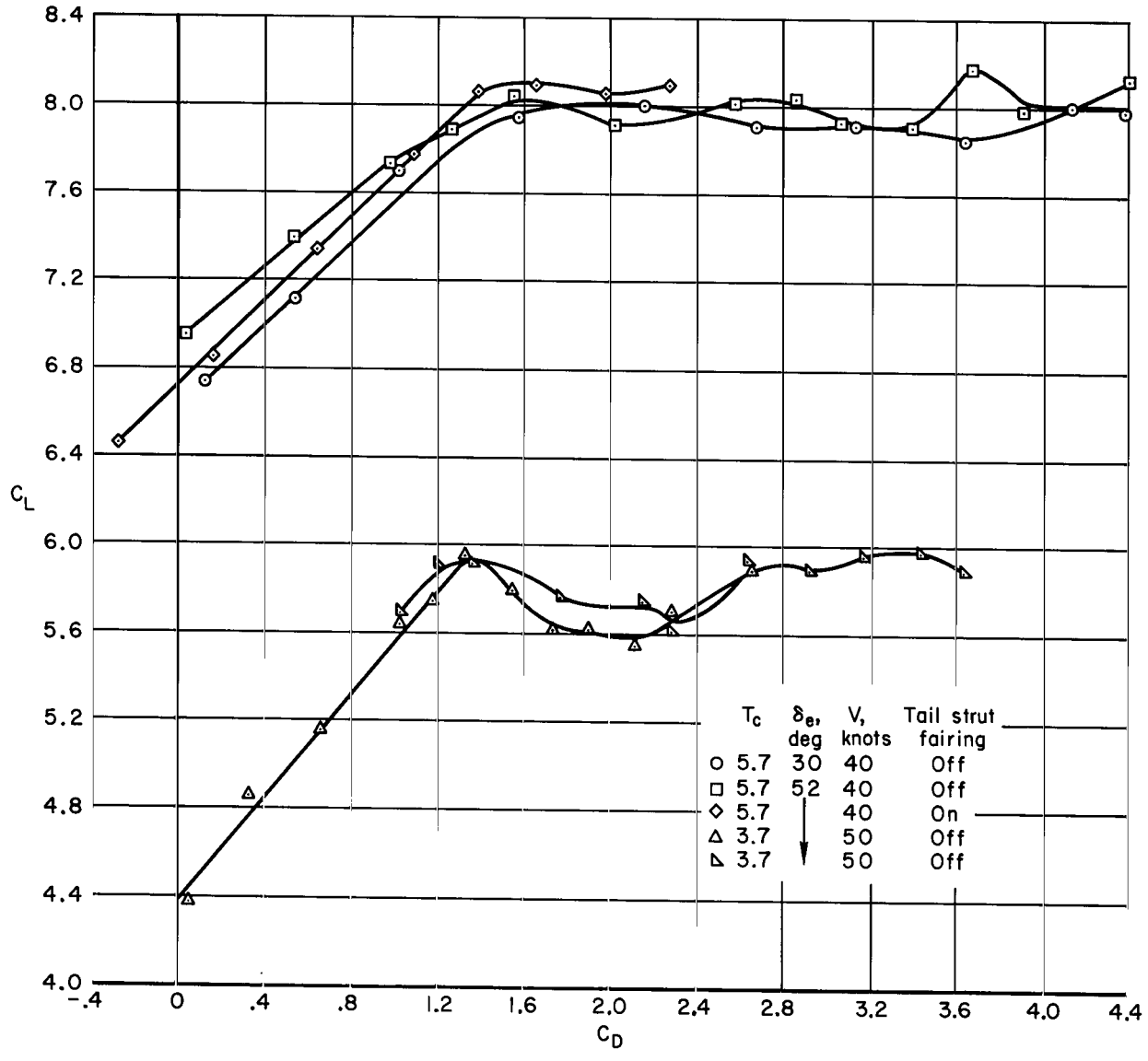

(b) C_L vs C_D

Figure 11.- Concluded.

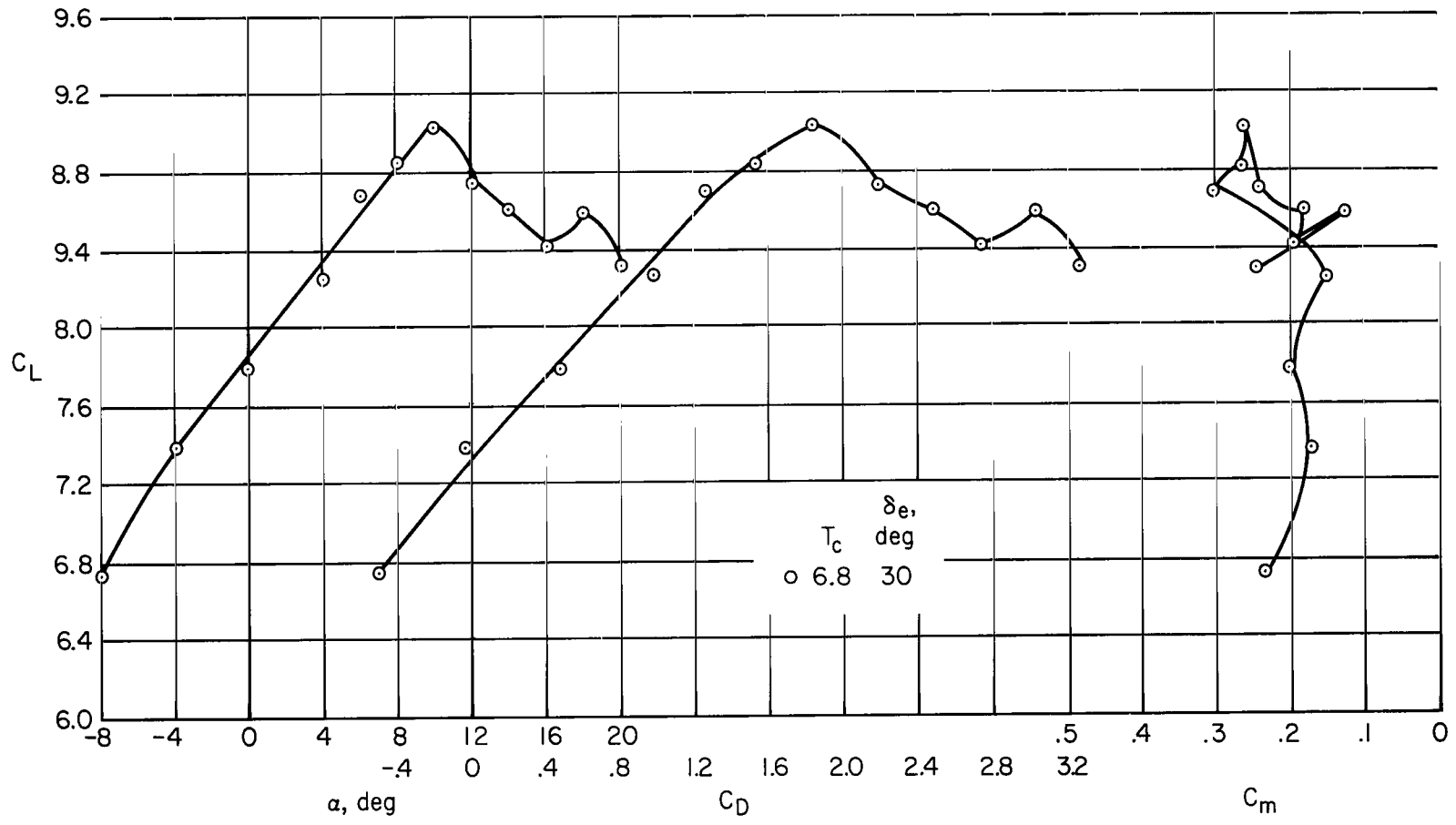

(a) V = 50 knots.

Figure 12.- Longitudinal characteristics in transition; configuration I, high power, $\delta_f = 40^\circ$.

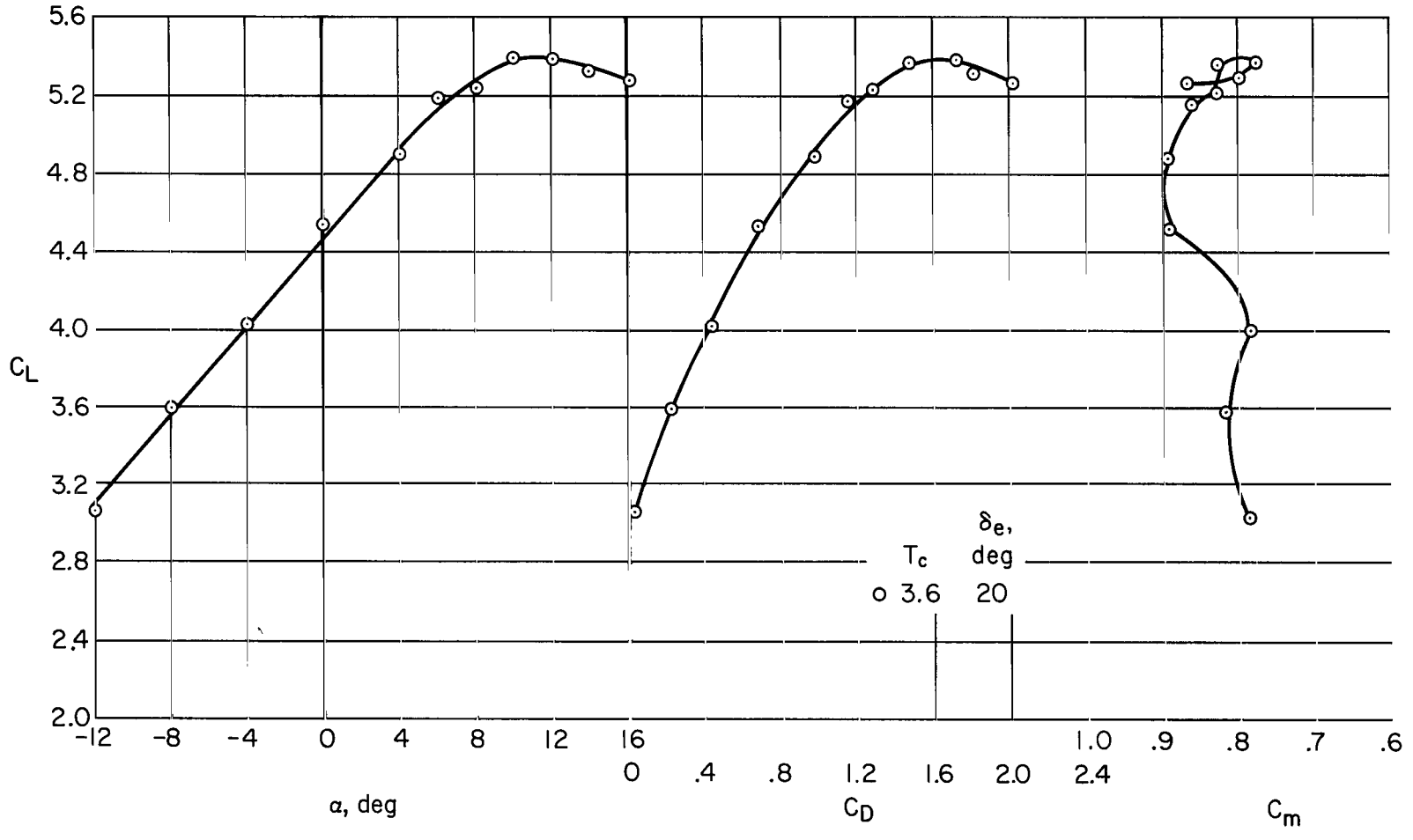

(b) V = 70 knots.

Figure 12.- Concluded.

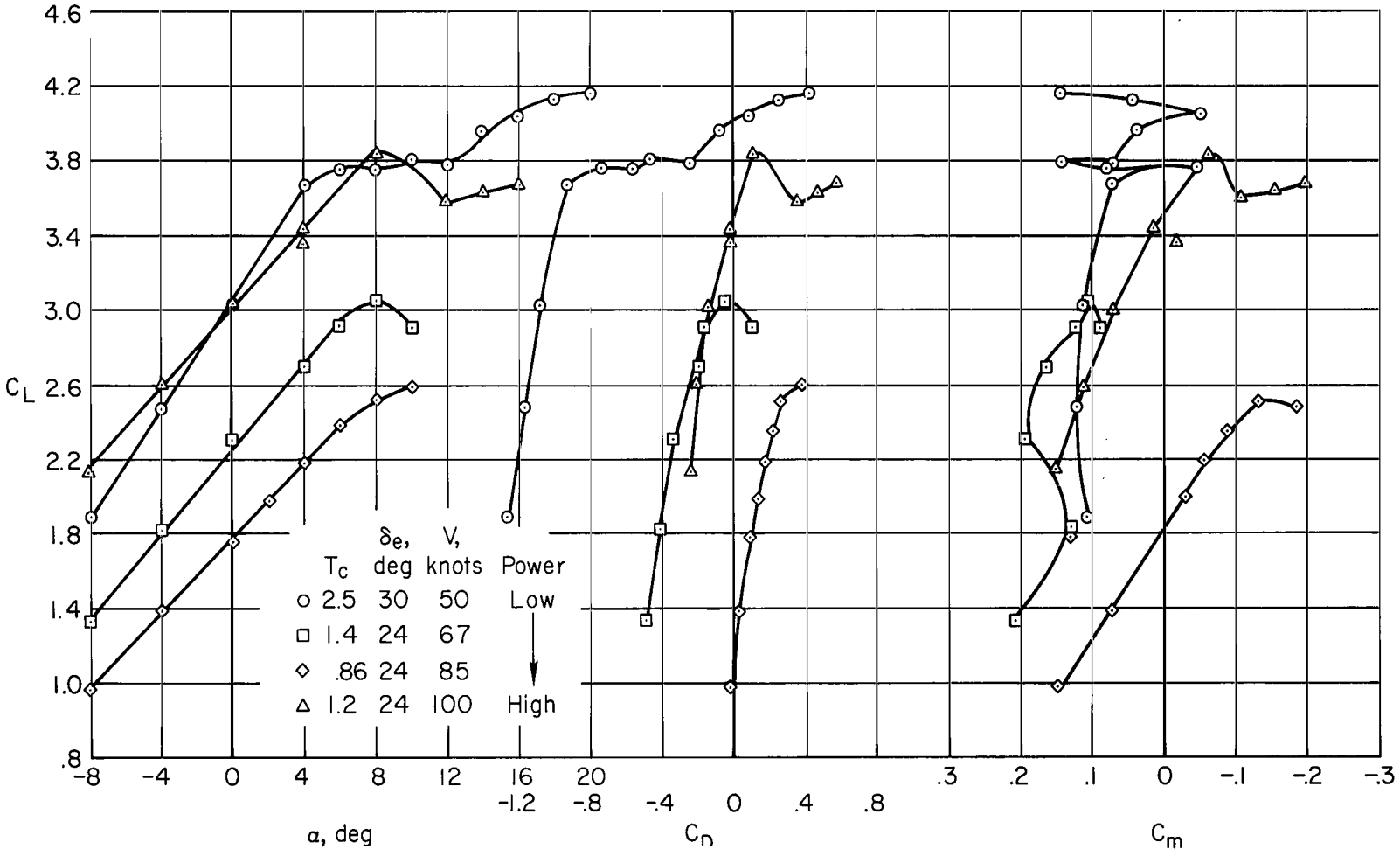

Figure 13.- Longitudinal characteristics in transition; configuration II, $\delta_f = 40^\circ$.

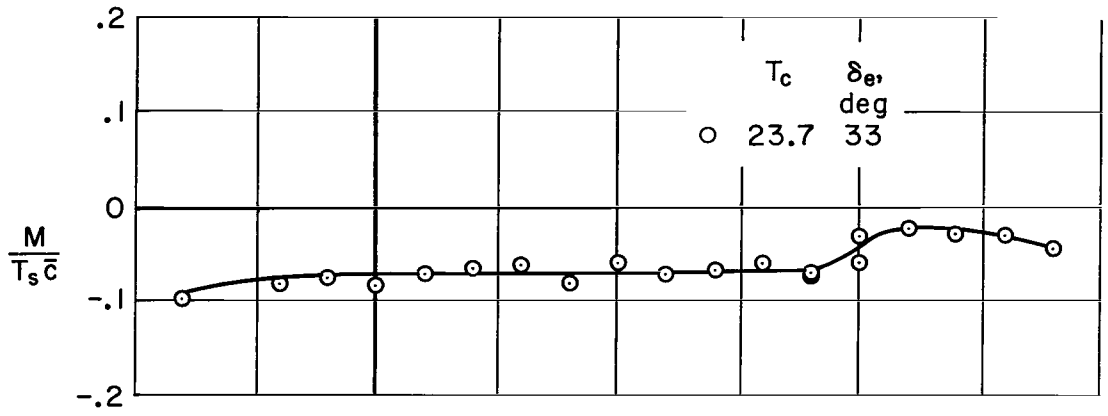

(a) V = 20 knots, low power.

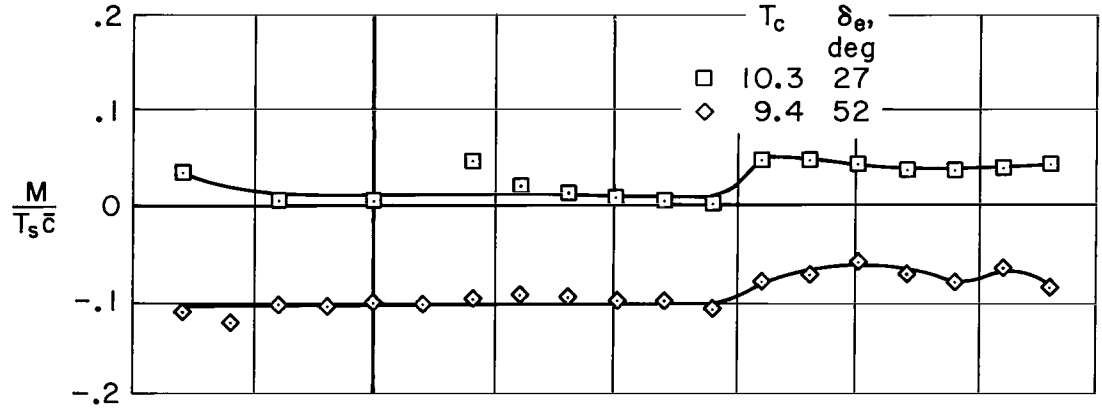

(b) V = 30 knots, low power.

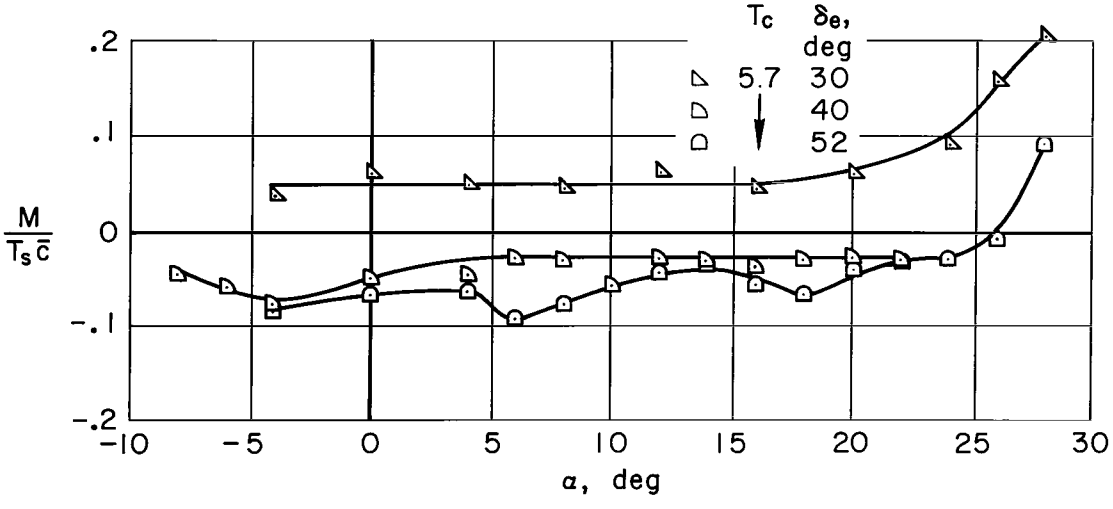

(c) V = 40 knots, low power.

Figure 14.- Longitudinal stability in transition; configuration I, $\delta_f = 40^\circ$.

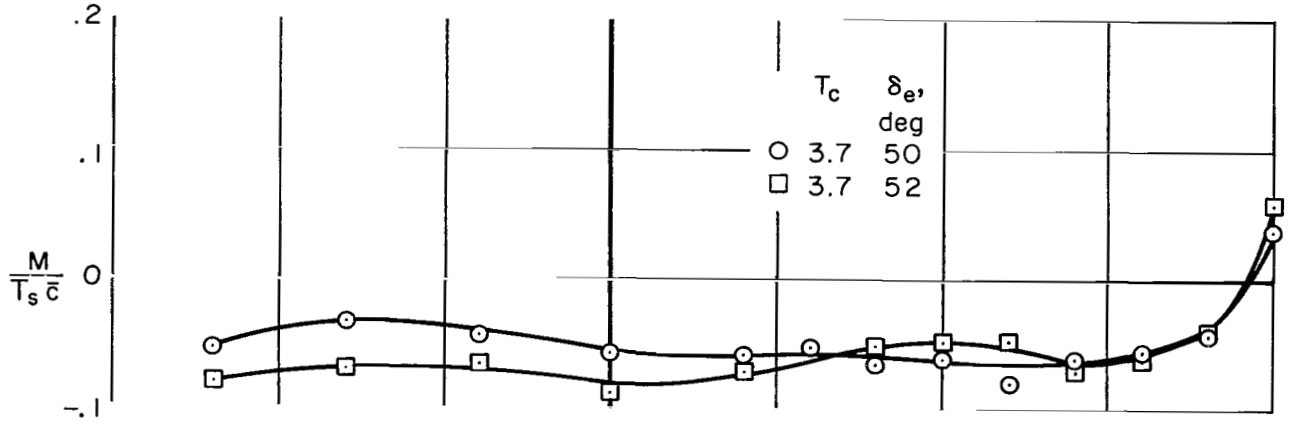

(d) V = 50 knots, low power.

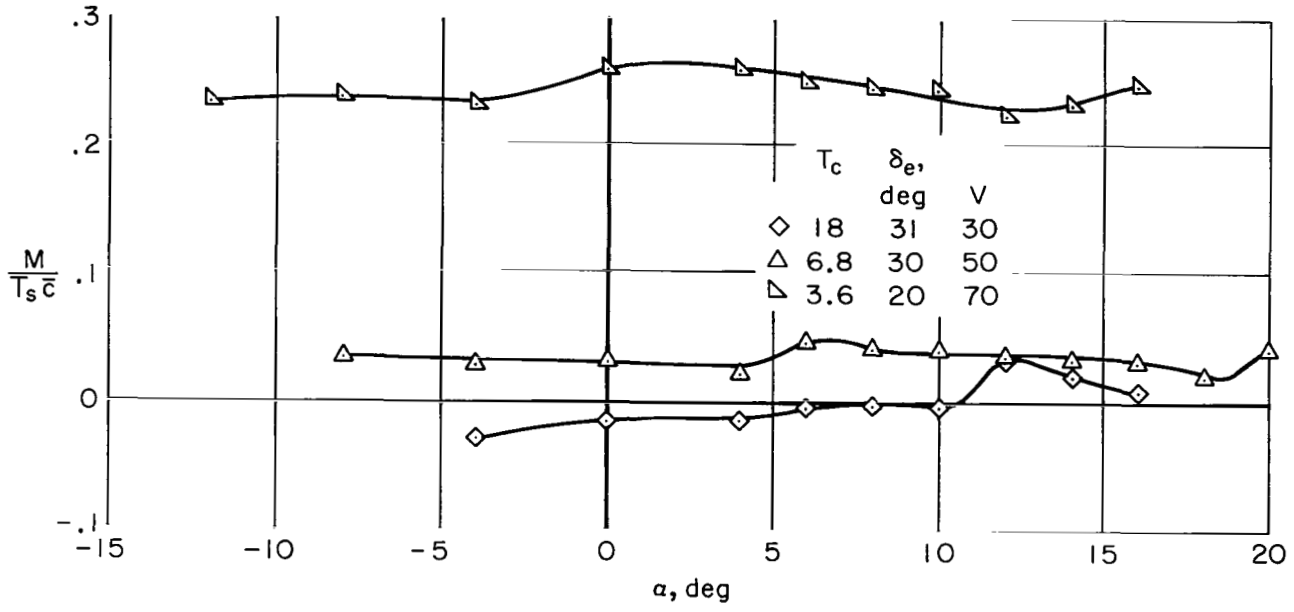

(e) High power.

Figure 14.- Concluded.

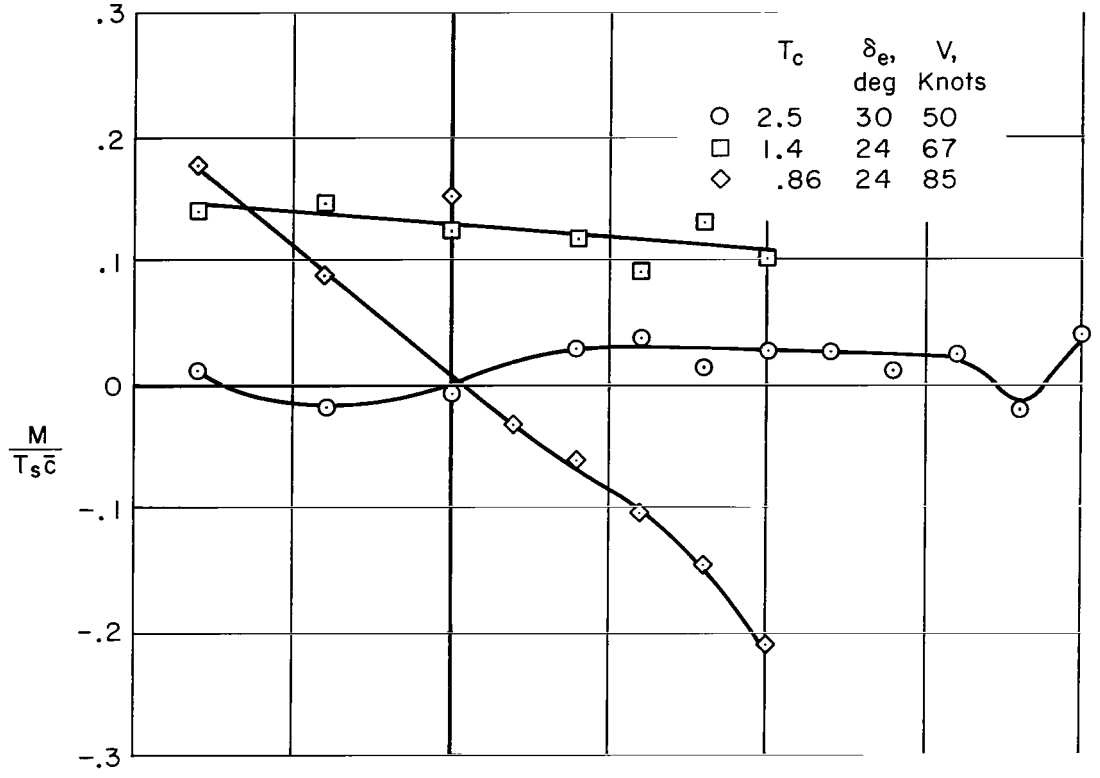

(a) Low power.

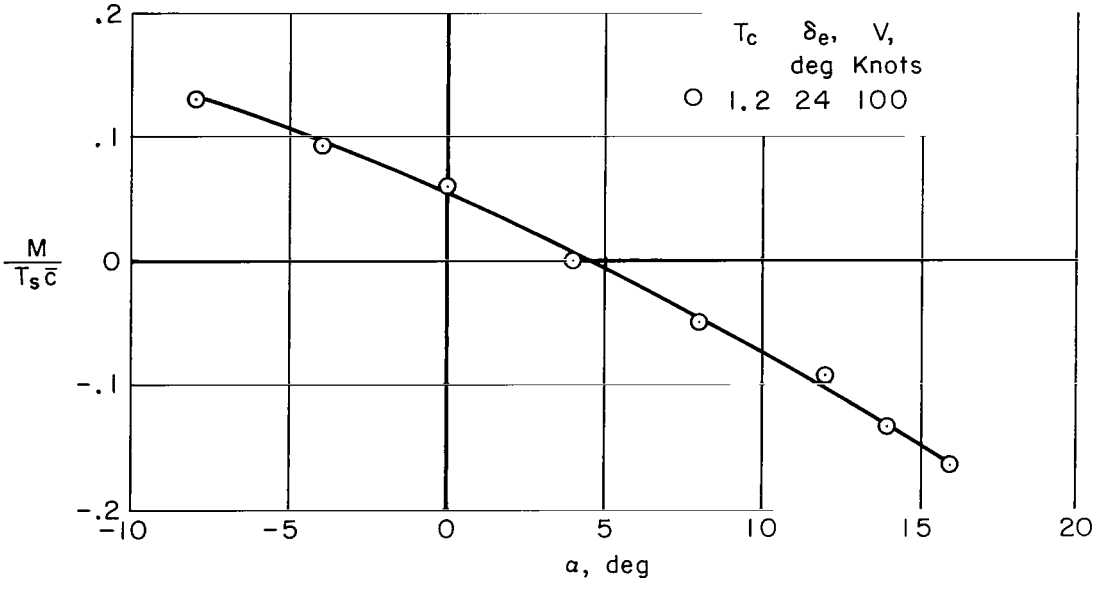

(b) High power.

Figure 15.- Longitudinal stability in transition; configuration II, $\delta_f = 40^\circ$.

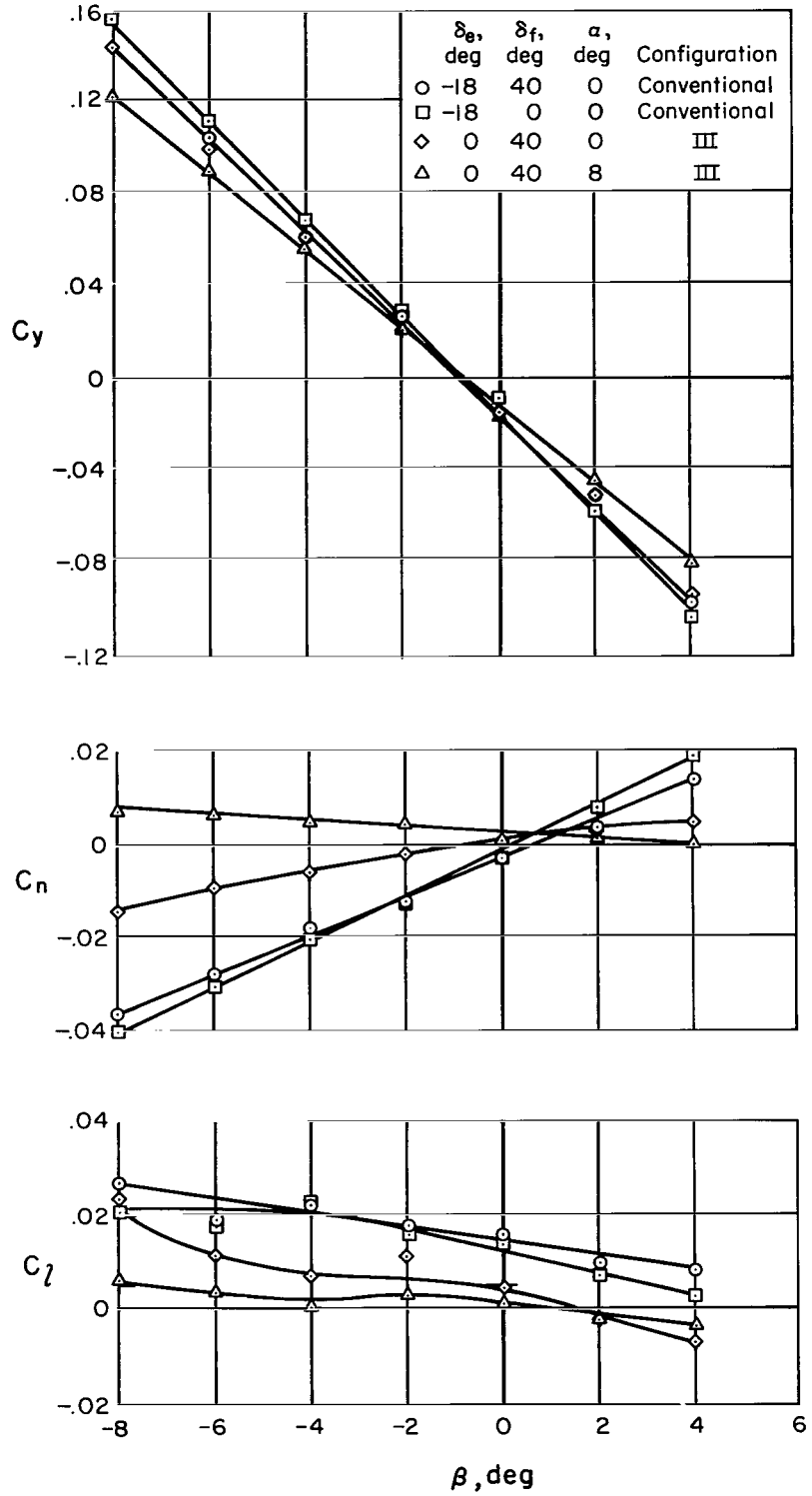

Figure 16.- Lateral-directional characteristics in transition; power off, V = 80 knots.

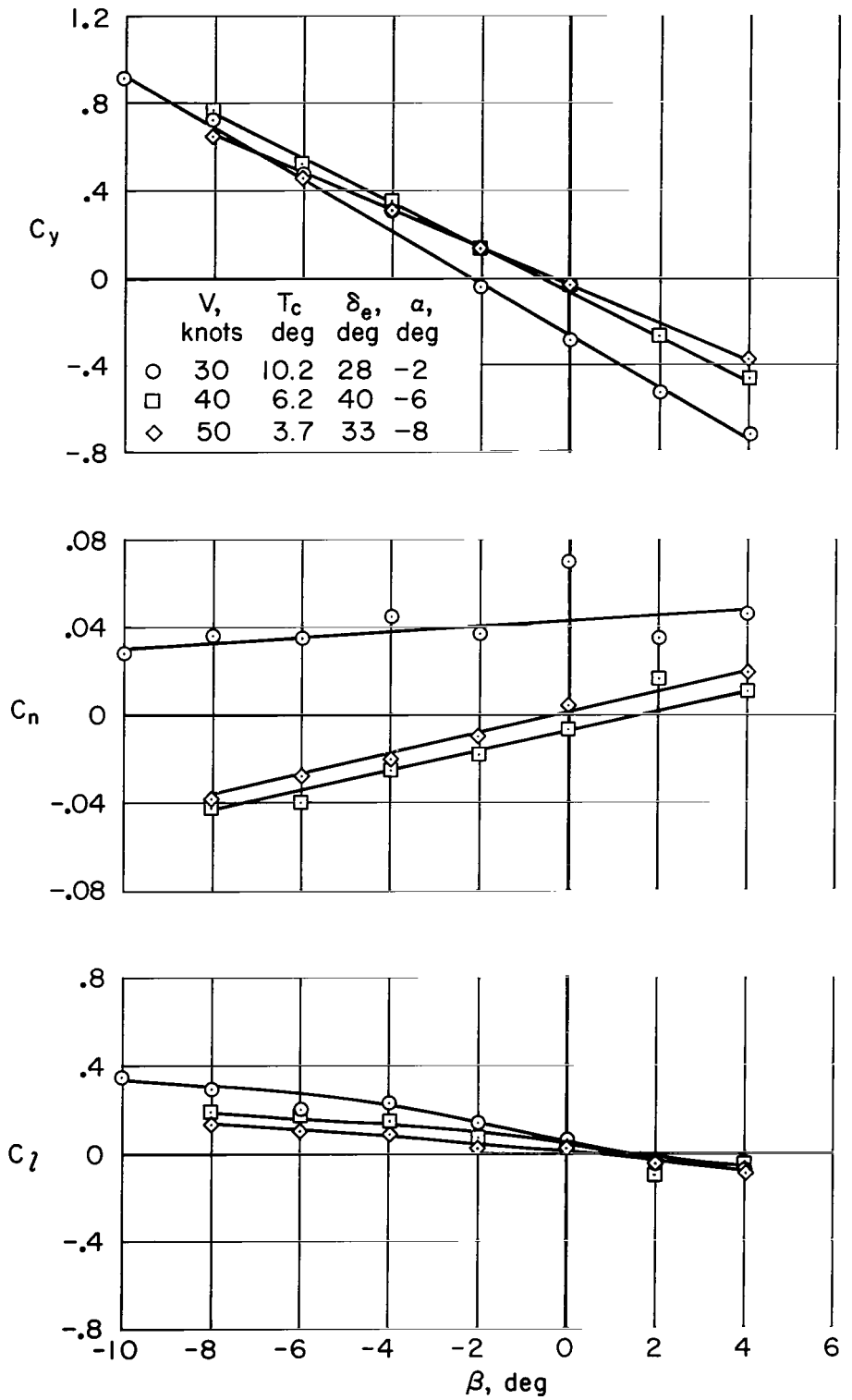

Figure 17.- Lateral-directional characteristics in transition; configuration I, low power, $\delta_f = 40^\circ$.

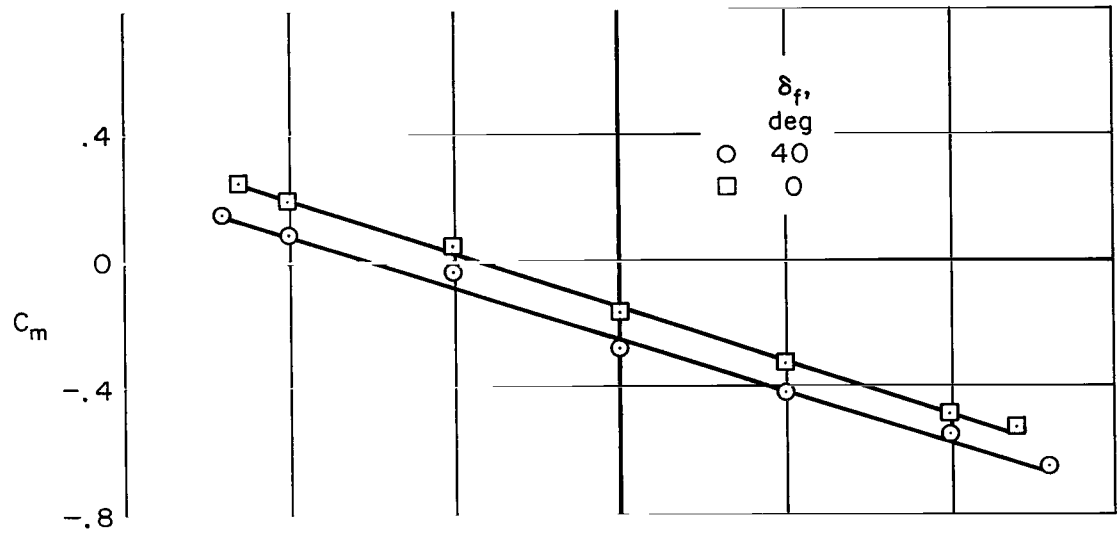

(a) Power off.

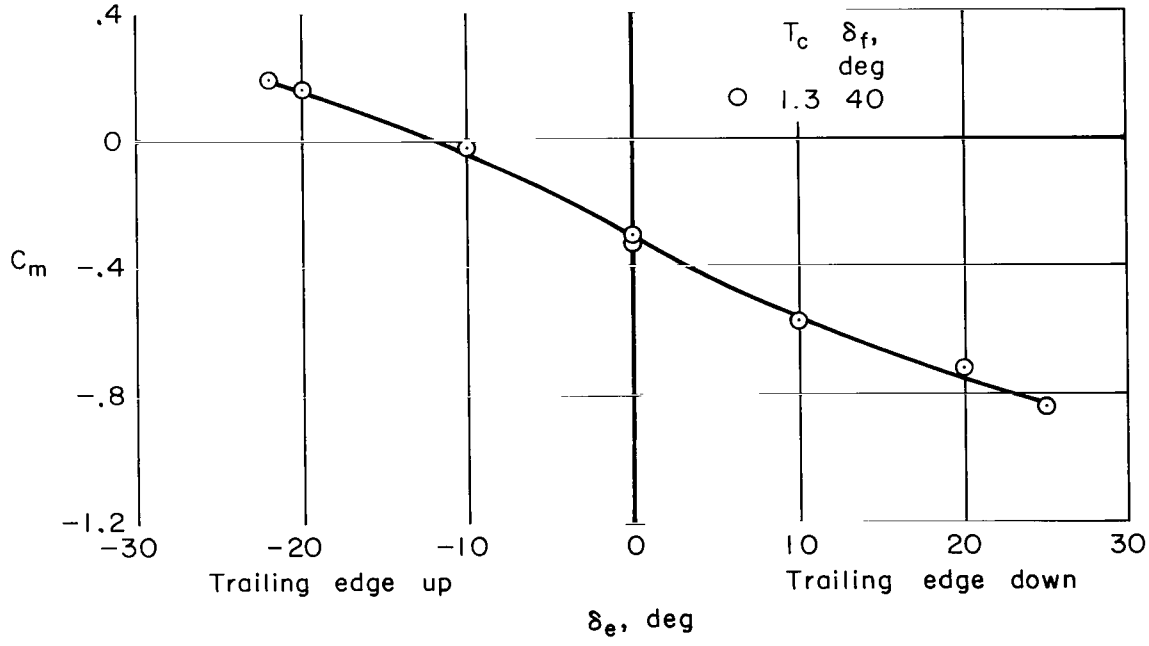

(b) Power on, low power.

Figure 18.- Longitudinal control power in the conventional flight configuration; V = 80, $\alpha = 0^o$, $\beta = 0^o$.

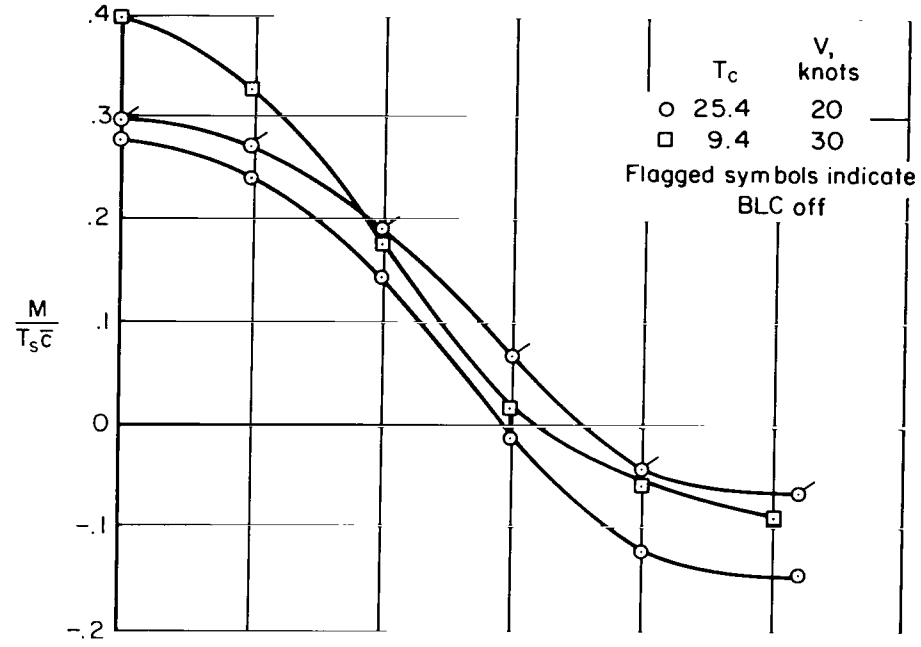

(a) Low power $\alpha = 0^{\circ}$.

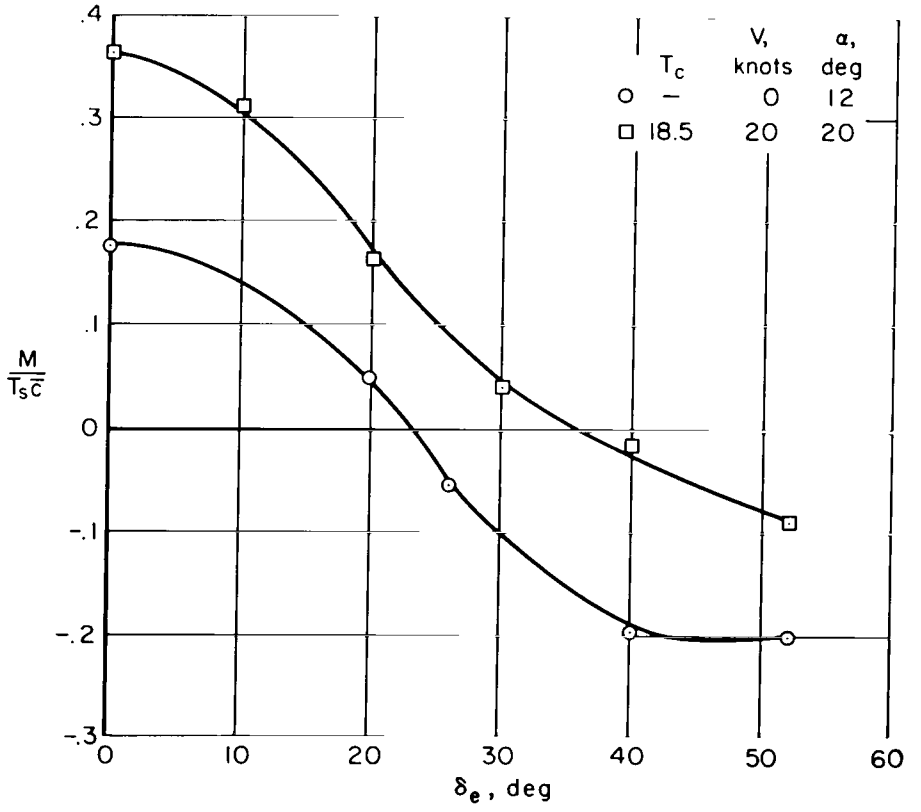

(b) High power.

Figure 19.- Longitudinal control power in transition; configuration I, $\delta_f = 40^{\circ}$, $\beta = 0^{\circ}$.

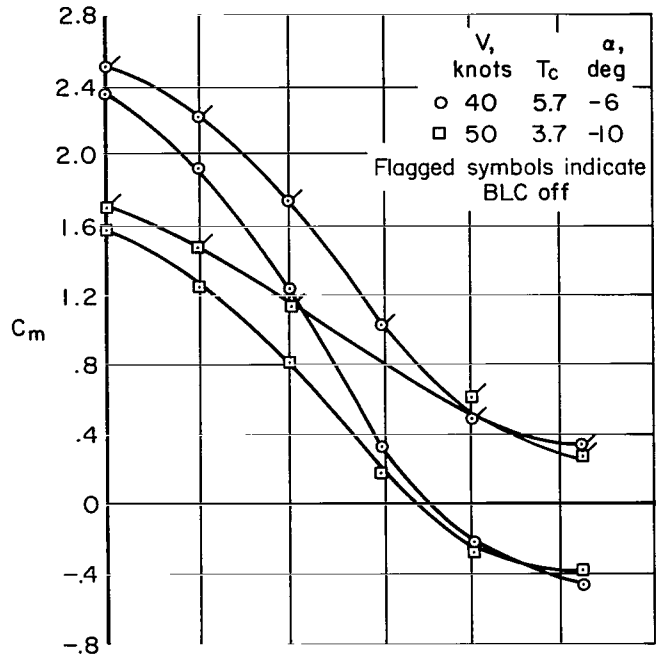

(a) Low power.

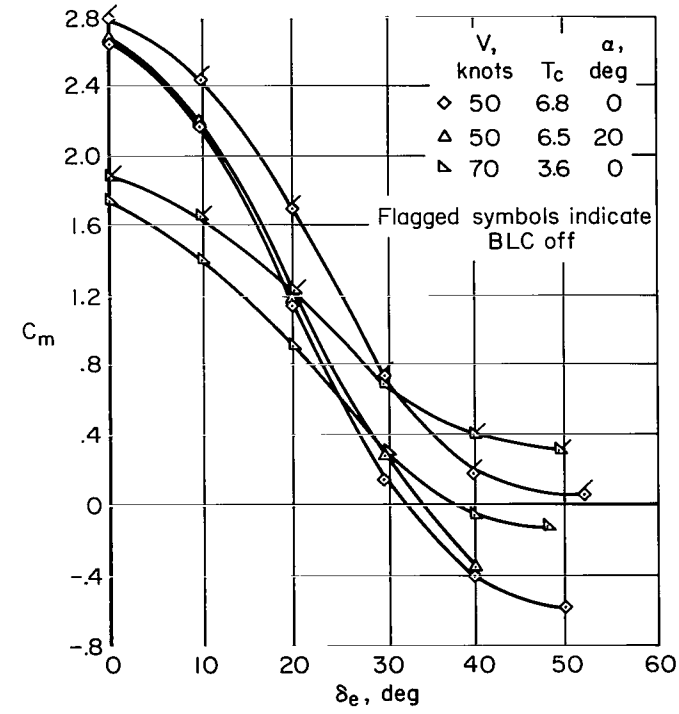

(b) High power.

Figure 20.- Longitudinal control power in transition; configuration I, $\delta_f = 40^\circ$, $\beta = 0^\circ$.

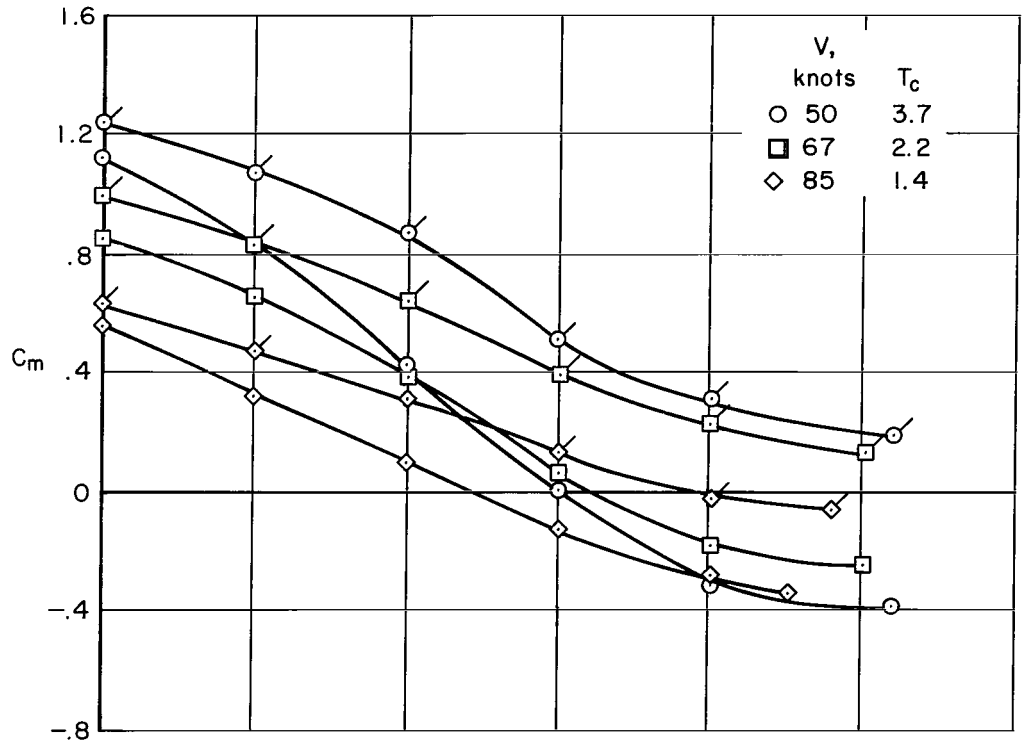

(a) Low power, $\alpha = 0^\circ$.

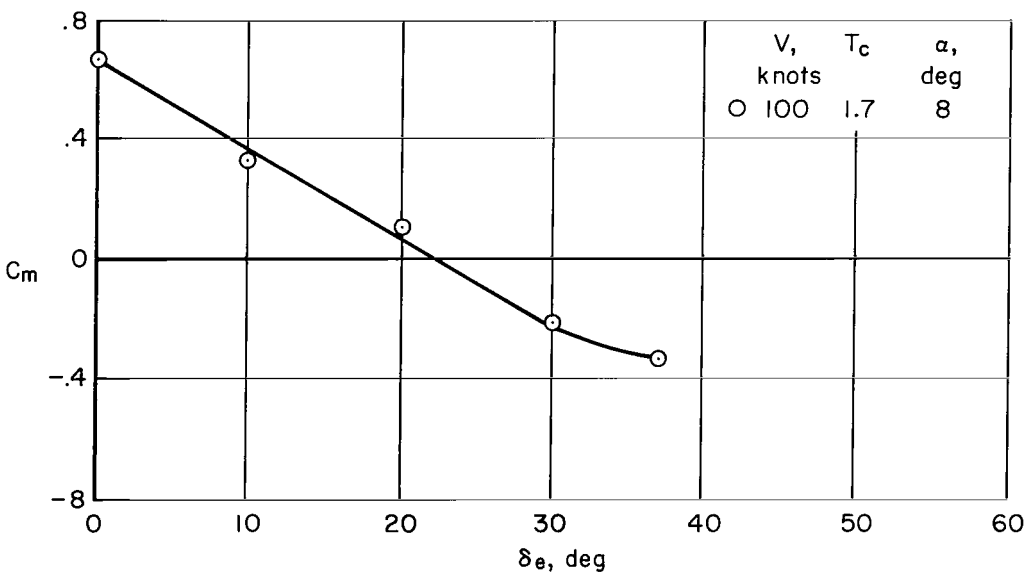

(b) High power.

Figure 21.- Longitudinal control power in transition; configuration II, $\delta_f = 40^\circ$, $\beta = 0^\circ$.

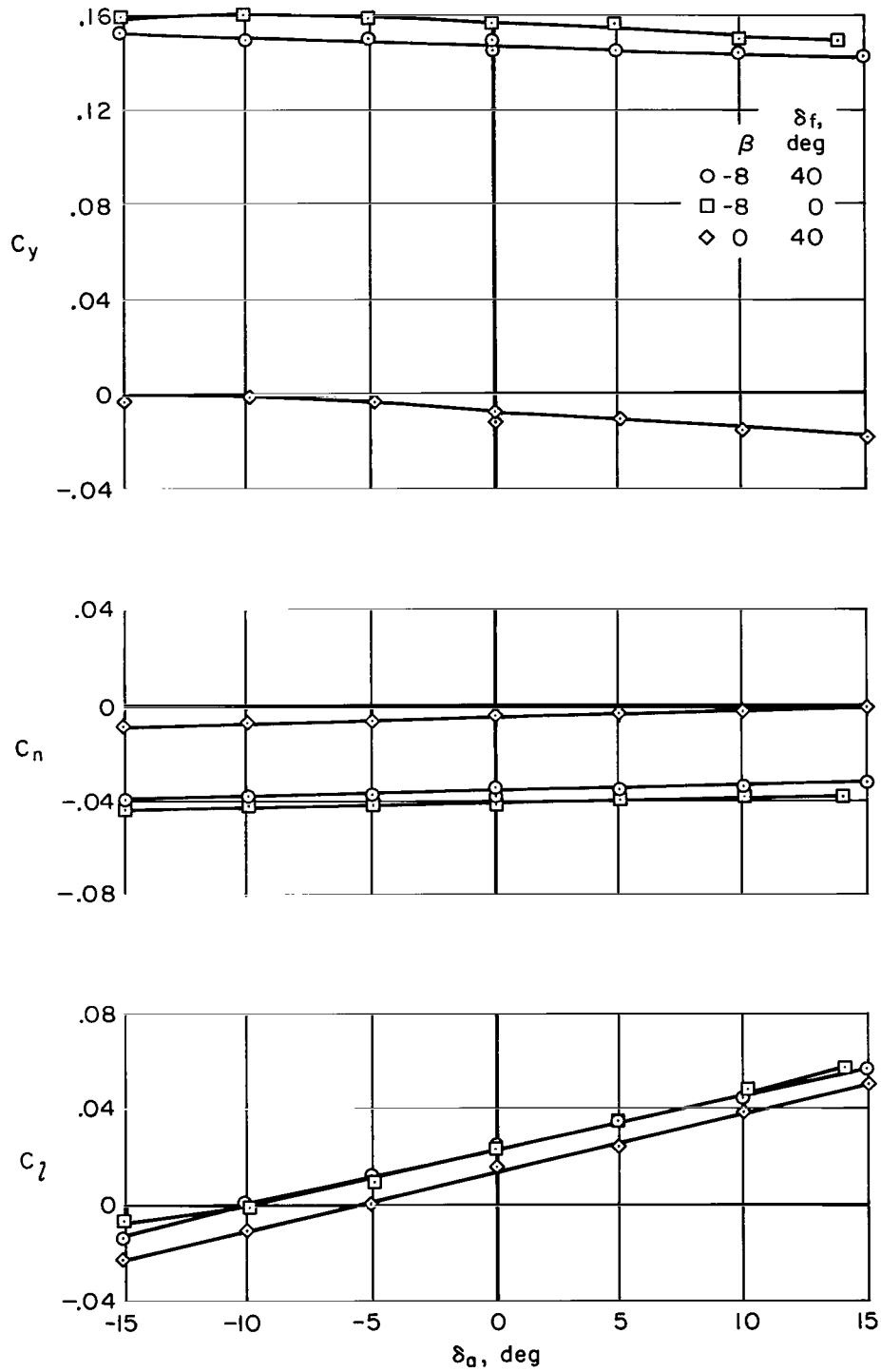

Figure 22.- The effect of sideslip and flap deflection on lateral control power in the conventional flight configuration; power off, V = 80 knots, $\delta_e = -18^\circ$, $\alpha = 0^\circ$.

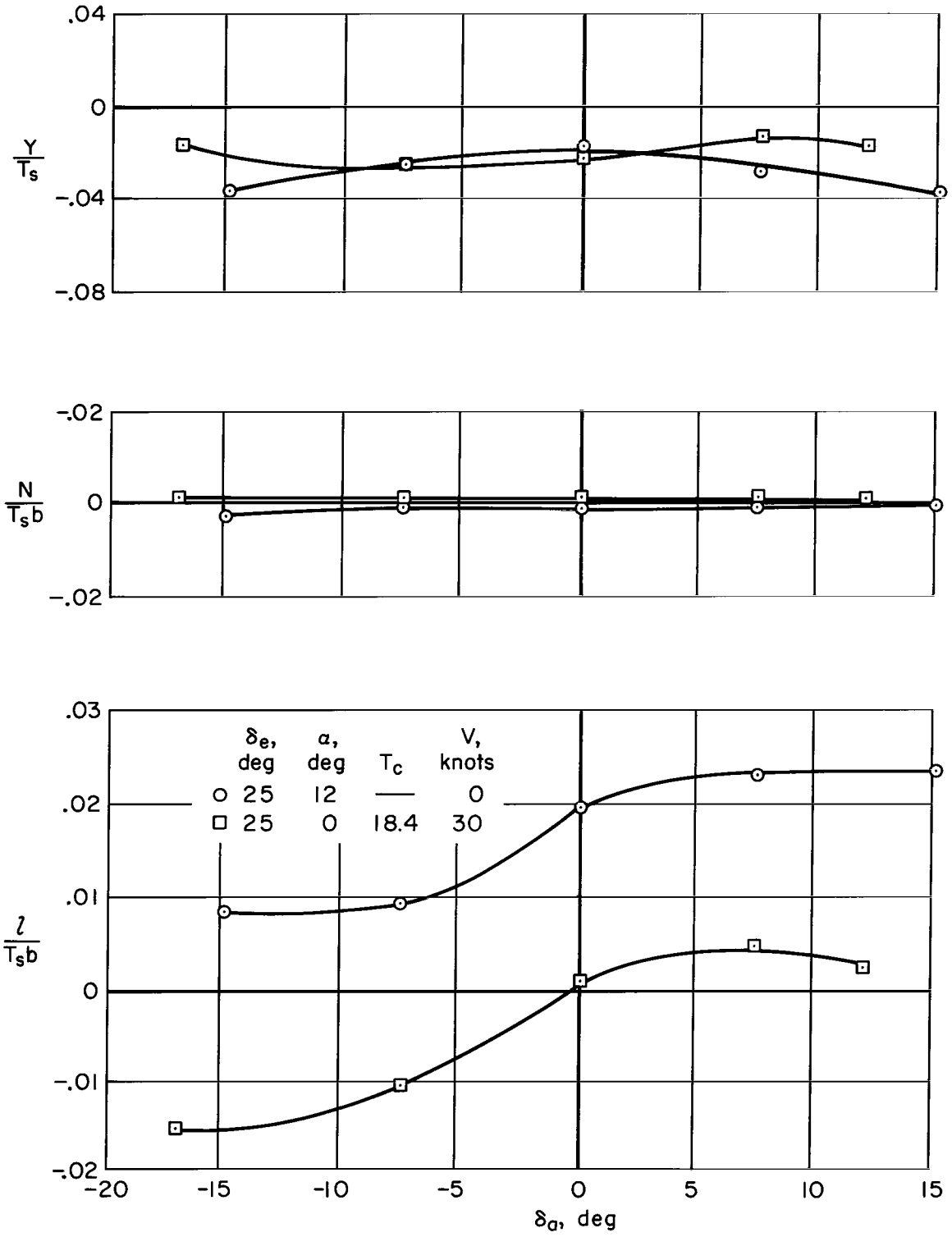

Figure 23.- Lateral control power in transition; configuration I, high power, $\delta_f = 40^\circ$, $\beta = 0^\circ$.

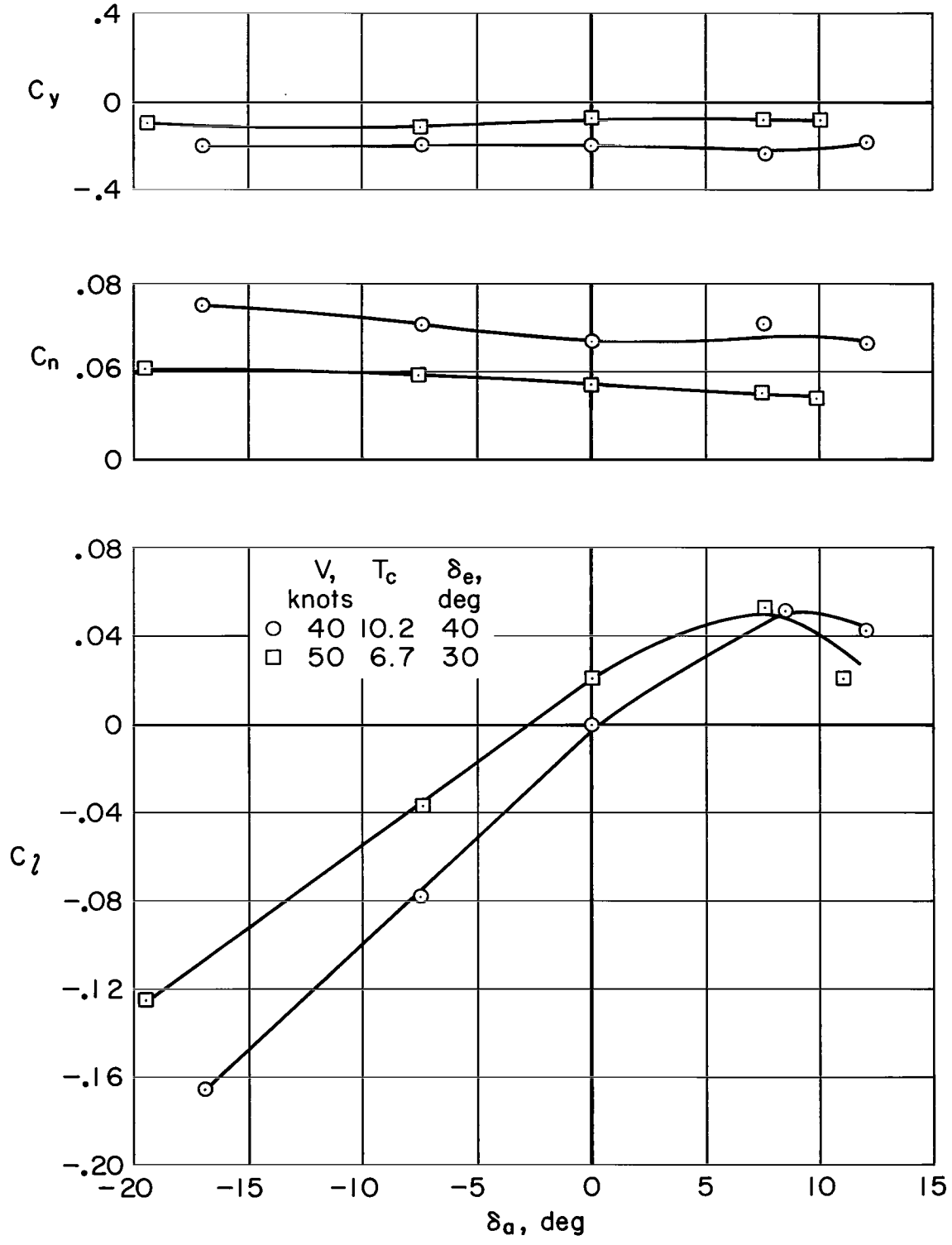

Figure 24.- Lateral control power in transition; configuration I, high power, $\delta_f = 40^\circ$, $\beta = 0^\circ$.

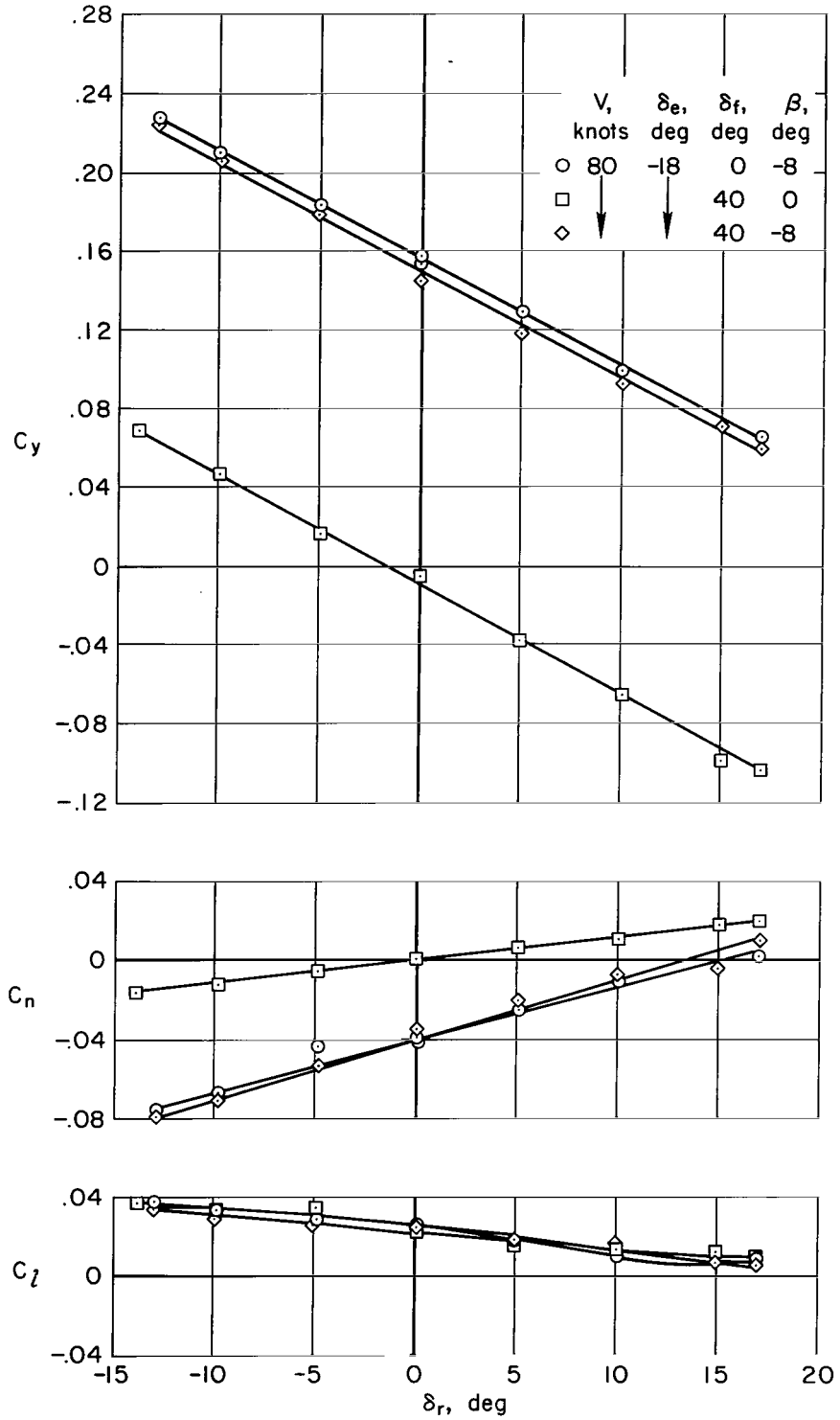

Figure 25.- Effect of sideslip and flap deflection on directional control power in the conventional flight configuration; power off V = 80 knots, $\alpha = 0^{\circ}$.

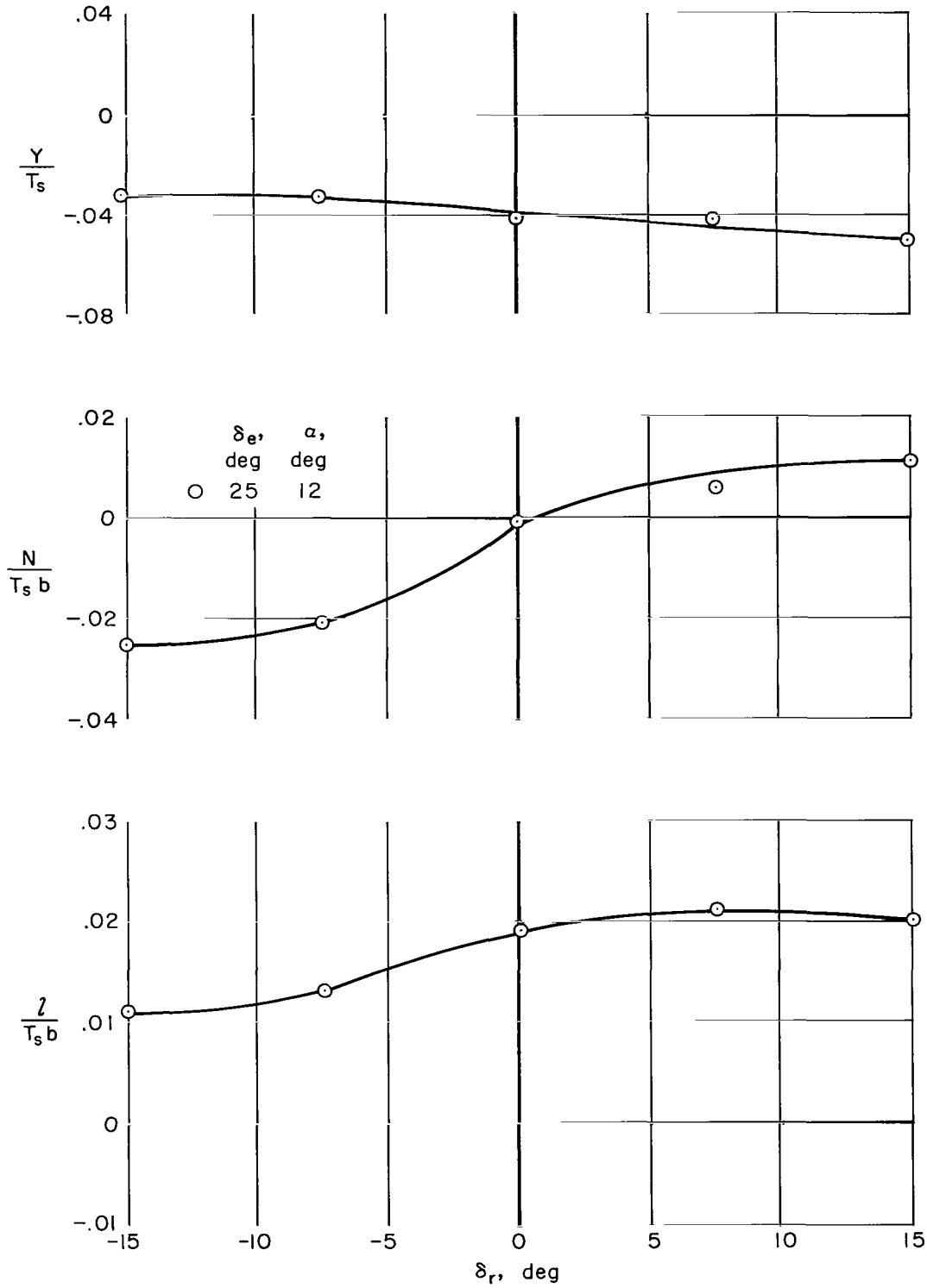

Figure 26.- Directional control power in hover; configuration I, high power, $V = 0$, $\delta_f = 40^\circ$, $\beta = 0^\circ$.

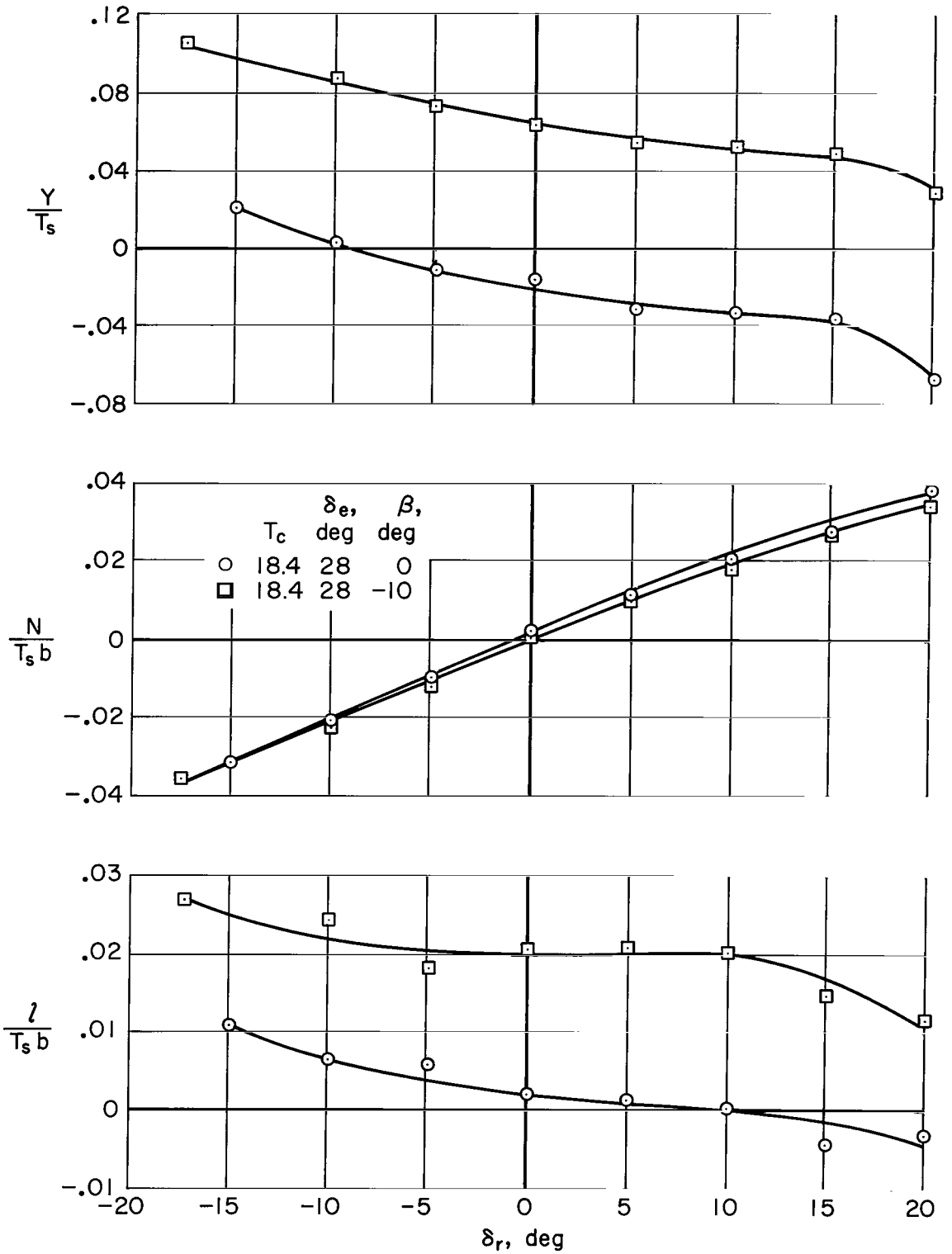

Figure 27.- Directional control power in transition; configuration I, low power, V = 20 knots, $\alpha = 0^{\circ}$, $\delta_f = 40^{\circ}$.

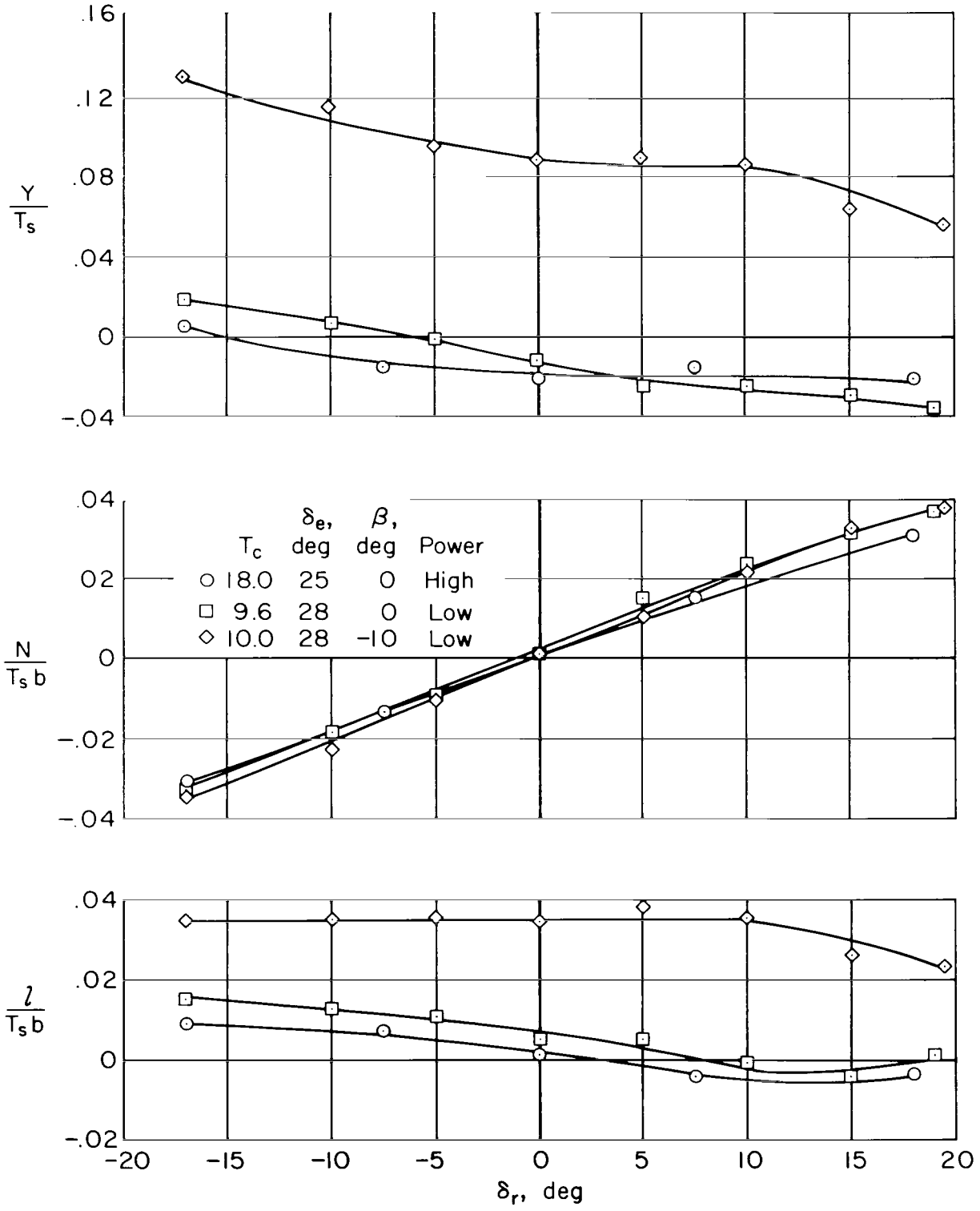

Figure 28.- Directional control power in transition; configuration I, V = 30 knots, $\alpha = 0^\circ$, $\delta_f = 40^\circ$.

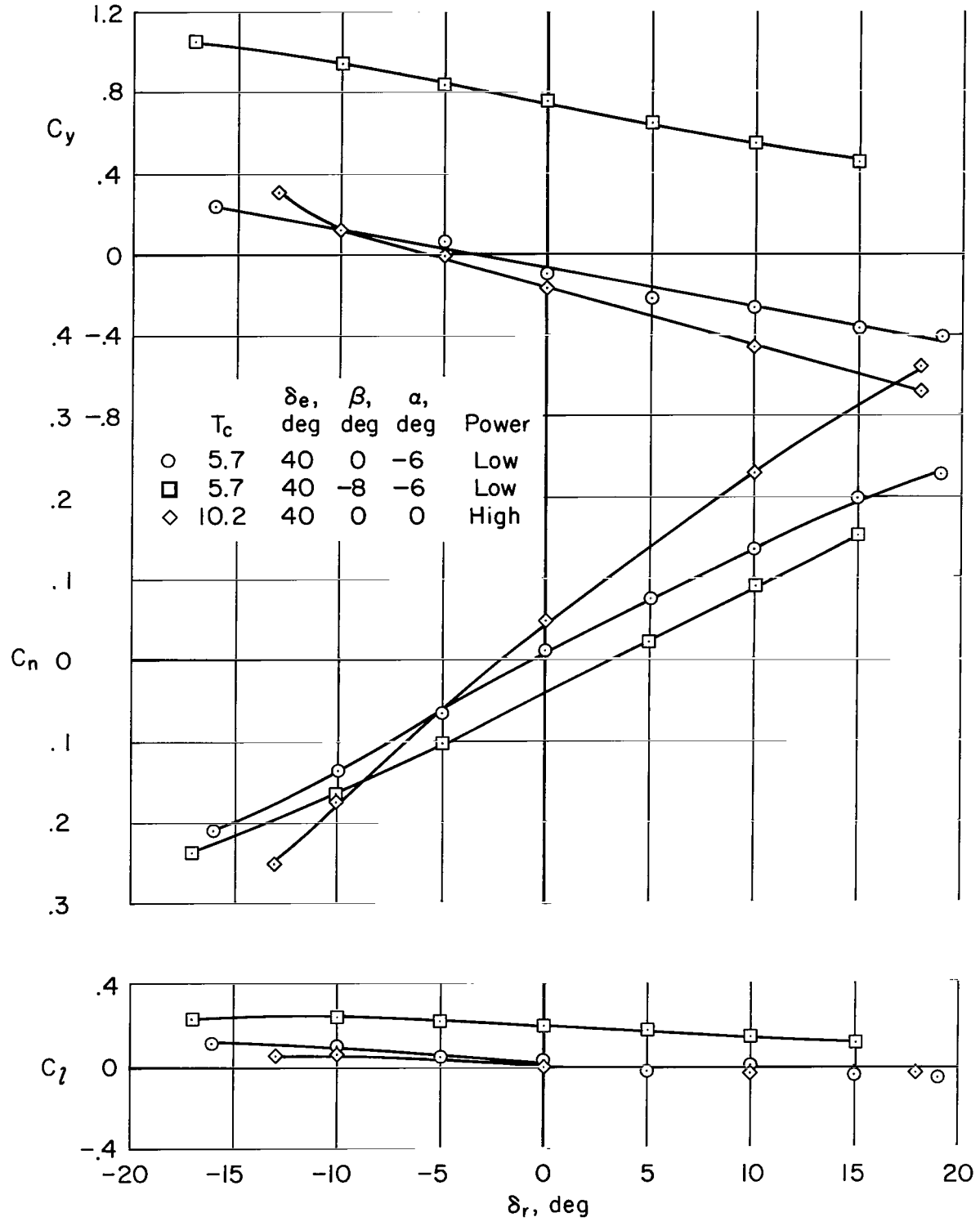

Figure 29.- Directional control power in transition; configuration I, V = 40 knots, $\delta_f = 40^\circ$.

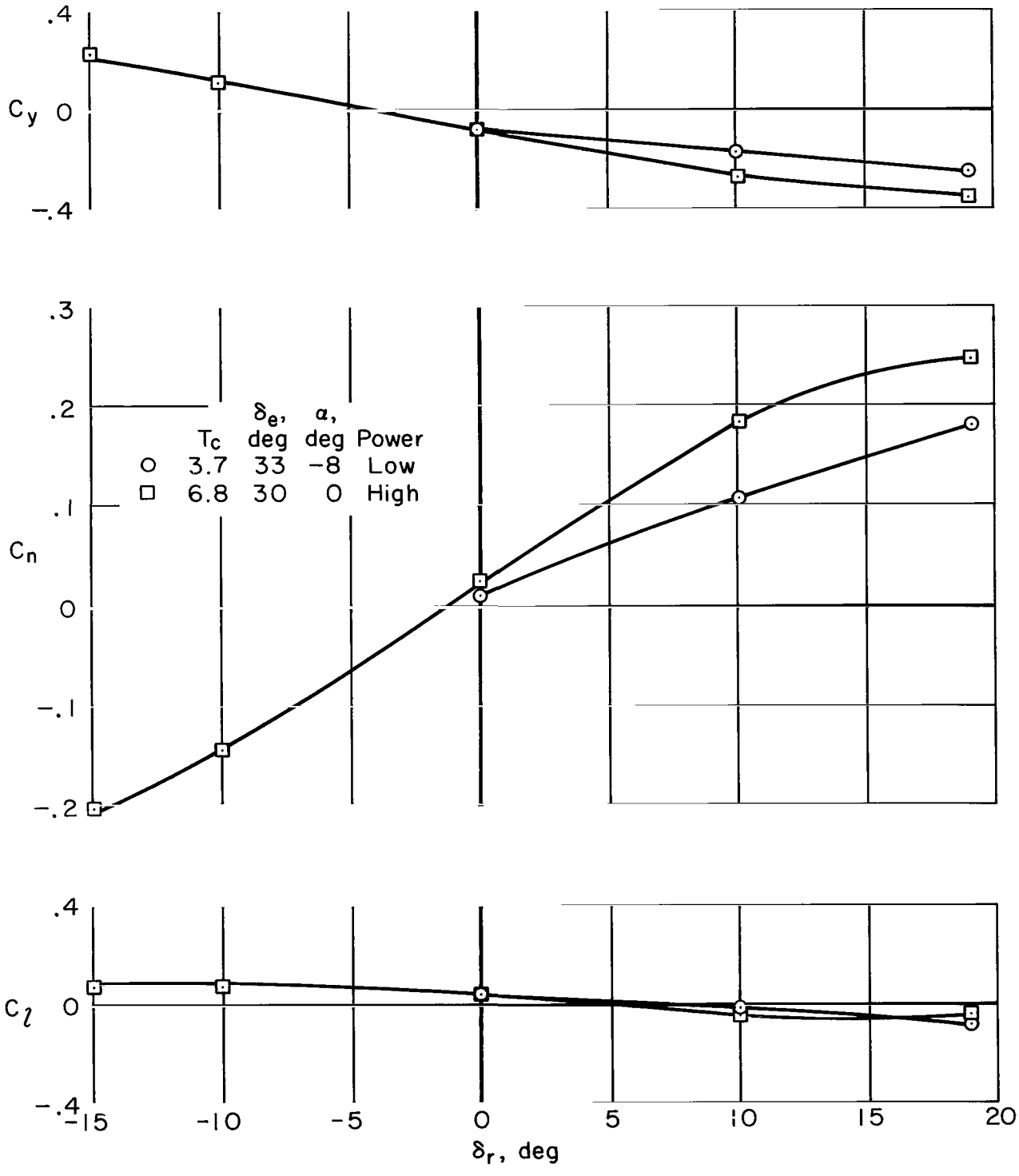

Figure 30.- Directional control power in transition; configuration I, V = 50 knots, $\delta_f = 40^\circ$, $\beta = 0^\circ$.

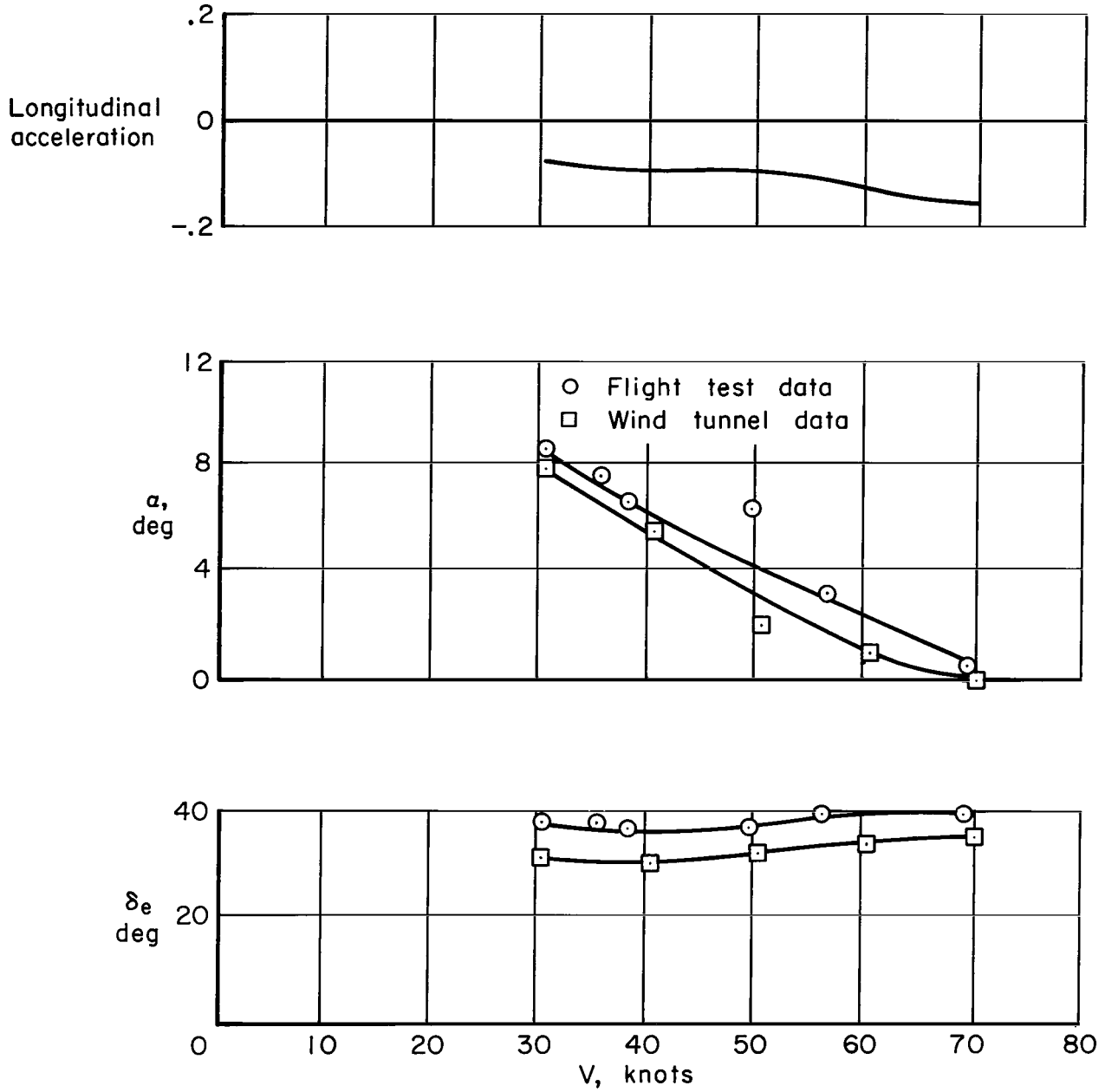

Figure 31.- Comparison of results between full-scale wind-tunnel and flight tests.

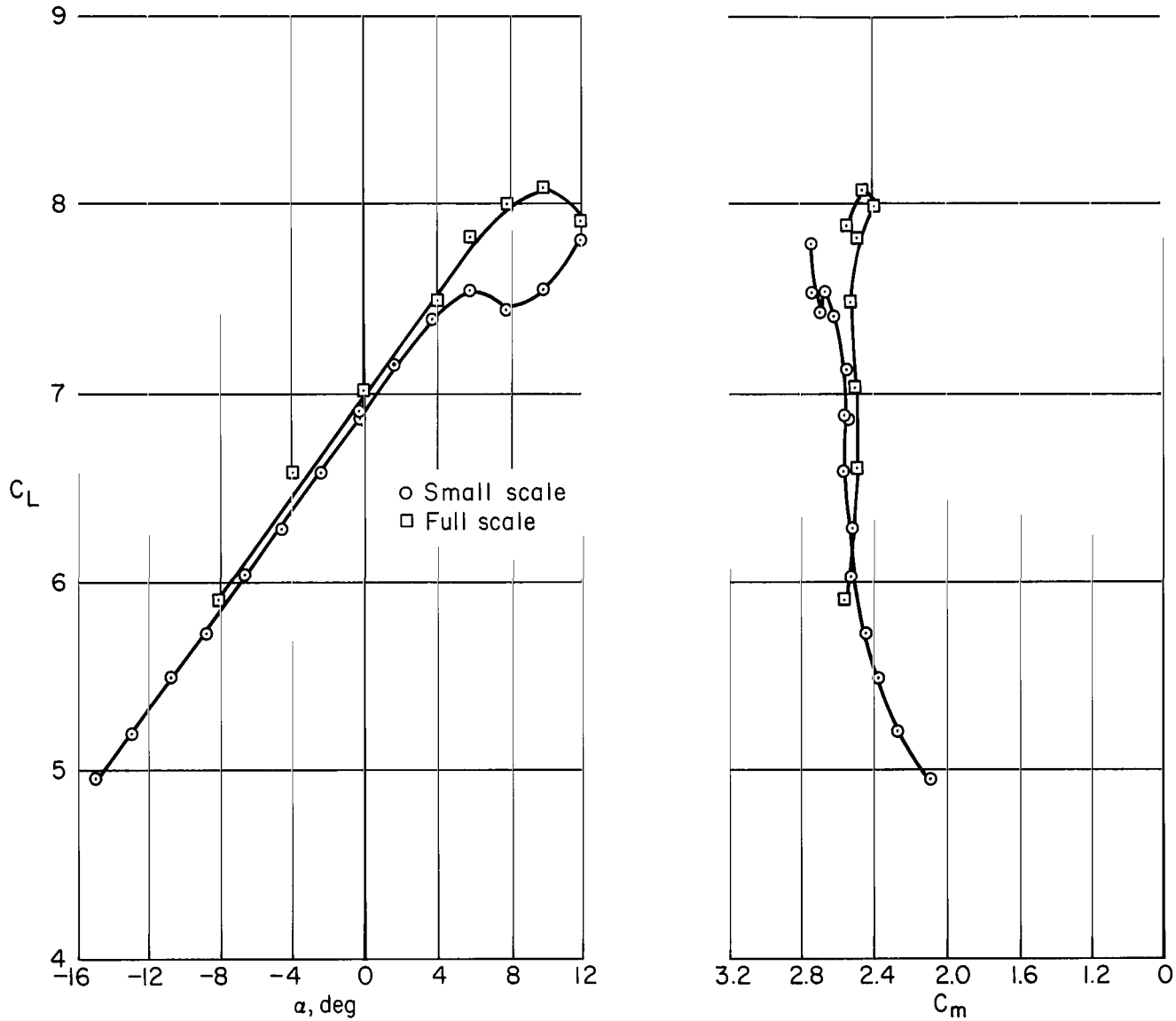

Figure 32.- Comparison of full-scale and small-scale (0.18) model wind-tunnel results; configuration I, $T_c = 6.25$, $\delta_f = 40^\circ$, $i_t = 0^\circ$, $\delta_e = 0^\circ$.

"The aeronautical and space activities of the United States shall be conducted so as to contribute . . . to the expansion of human knowledge of phenomena in the atmosphere and space. The Administration shall provide for the widest practicable and appropriate dissemination of information concerning its activities and the results thereof."

—NATIONAL AERONAUTICS AND SPACE ACT OF 1958

NASA SCIENTIFIC AND TECHNICAL PUBLICATIONS

TECHNICAL REPORTS: Scientific and technical information considered important, complete, and a lasting contribution to existing knowledge.

TECHNICAL NOTES: Information less broad in scope but nevertheless of importance as a contribution to existing knowledge.

TECHNICAL MEMORANDUMS: Information receiving limited distribution because of preliminary data, security classification, or other reasons.

CONTRACTOR REPORTS: Technical information generated in connection with a NASA contract or grant and released under NASA auspices.

TECHNICAL TRANSLATIONS: Information published in a foreign language considered to merit NASA distribution in English.

TECHNICAL REPRINTS: Information derived from NASA activities and initially published in the form of journal articles.

SPECIAL PUBLICATIONS: Information derived from or of value to NASA activities but not necessarily reporting the results of individual NASA-programmed scientific efforts. Publications include conference proceedings, monographs, data compilations, handbooks, sourcebooks, and special bibliographies.

Details on the availability of these publications may be obtained from:

SCIENTIFIC AND TECHNICAL INFORMATION DIVISION

NATIONAL AERONAUTICS AND SPACE ADMINISTRATION

Washington, D.C. 20546